

بِسْمِ اللَّهِ الرَّحْمَنِ الرَّحِيمِ



*Sudan University of Science and Technology*

*College of Post Graduate Studies*



**Modeling QSAR, Docking and Grinding Preparation of Some  
3.5 Pyrazoline Derivatives, Against AsPC-1 Human Pancreatic  
Cell Line and U251 Human Glioblastoma Cell Line**

النمذجة والعلاقة الكمية بين البنية الجزيئية والفعالية والإرساء والتحضير الطحني  
لبعض مشتقات البايرازولين ضد سرطان البنكرياس والدماغ

*By:*

**Nihad Abdelrahman Adam Abdelrahman**

A thesis submitted for the partial fulfillment of the requirement  
of the M.Sc. degree in chemistry

*Supervisor:*

**Prof. Dr. Ahmed Elsadig Mohammed Saeed**

**March 2019**

بِسْمِ اللّٰهِ الرَّحْمٰنِ الرَّحِیْمِ

## الآية

قال تعالي :

﴿ إِنَّا عَرَضْنَا الْأَمَانَةَ عَلَى السَّمَاوَاتِ وَالْأَرْضِ وَالْجِبَالِ فَأَيُّنَ أَنْ  
يَحْمِلْنَهَا وَأَشْفَقْنَ مِنْهَا وَحَمَلَهَا الْإِنْسَانُ إِنَّهُ كَانَ ظَلُومًا جَهُولًا ﴾.

صدق الله العظيم

سورة الأحزاب الآية (72)

## *Dedication*

I Dedicate this work with deep love and respect to

My Family

And to

My friends

## *Acknowledgement*

Thanks to **ALLAH** the most gracious, the compassionate for given me strength and health to complete this work.

I would like to specially thank my supervisor, Prof. Dr. Ahmed Alsadig, for the patient guidance, encouragement and advice he has provided throughout my time as his student. I have been extremely lucky to have a supervisor who cared so much about my work, and who responded to my questions and queries so promptly.

I would like also to acknowledge everyone who played role in my academic accomplishment. First of all, my family who supported me with love and understanding. Secondly, I wish to express my sincere thanks to all faculty members of the department of Chemistry, for providing me with all necessary facilities.

## *Abbreviations*

AM_1	Austin Model 1
ASA_H	Total hydrophobic surface area
F.Wt	Formula Weight
HOMO	Highest Occupied Molecular Orbital
IR	Infra-Red
Log p	log octanol/water partition coefficient
LUMO	Lowest unoccupied Molecular Orbital
M.F	Molecular Formula
M.P	Melting point
M.Wt	Molecular Weight
MLR	Multi Linear Regression
MR	Molar Refractivity
N.O	Number
P-Value	Probability Value
QSAR	Quantitative Structure Activity Relationship
RF	Retention Factor
S	Sample standard deviation
TLC	Thin Layer Chromatography
U.V	Ultra Violet
VSA	Van Der Waals Surface Area

## ***Abstract***

The QSAR model were successfully developed to calculate biological activity of 3, 5 di-substituted Pyrazoline derivatives as anticancer agents against AsPC-1 human pancreatic cell line and U251 human glioblastoma cell line, a good correlation models were obtained with  $R^2=74.30\%$  and  $R^2=75.92\%$  respectively, compounds (5-(4-bromophenyl)-3-(4-nitrophenyl)-4,5-dihydro-1H-pyrazole) and (N, N-dimethyl-4-[3-(4-nitrophenyl)-4,5-dihydro-1H-pyrazol-5-yl] aniline) were found to be the most effective anticancer agent against AsPC-1 and U251 cell lines, with  $IC_{50}$  values 0.31mM and 0.062mM respectively.

Series of 3, 5 di-substituted Pyrazoline derivatives were successfully synthesized in two steps under solvent free condition, which verify one of goals of green chemistry is the use of less hazardous solvents. Step one was synthesized enone by condensing aldehyde with ketone via sodium hydroxide according to Claisen-Schmidt condensation. Step two was a nucleophilic addition of hydrazine hydrate to enon. The structures of these compounds have been elucidated by infra red, ultra violet, thin layer chromatography and Melting Point.

## الخلاصة

تم حساب النشاط البيولوجي لمشتقات مركبات 3,5 بايرازولين ضد سرطان البنكرياس و سرطان الدماغ عن طريق ايجاد العلاقة بين النشاط البيولوجي والخصائص الفيزيائية او الفيزيوكيميائية لمركبات لها نفس التركيبة البنائية. كما تم ايضا تقييم فعاليتها من خلال دراسة ارتباط هذه المركبات مع بعض البروتينات المسببة للمرض . حيث وجد ان المركب (5-4-برمو فينيل)-3-4-نايترو فينيل)-4,5-ثنائي الهيدروجين- بايرازولين) و مركب (ثنائي الميثيل-4-3,4-نايترو فينيل)-4,5-ثنائي الهيدروجين بايرازول-5-يل] انيلين هما الاكثر فاعلية ضد سرطان البنكرياس و الدماغ بقيمة فاعلية تبلغ 0.31 ملي مول و 0.062 ملي مول علي الترتيب.

سبعة من مشتقات مركبات البايرازولين تمت تخليقها بواسطة تكاثف الالدهيد مع الكيتون في وسط قاعدي لتكون مركبات الكاربونيل الغير مشبعة.ومن ثم الاضافة النيوكليفية لسلفات الهيدرازين الي مركبات الكاربونيل غير المشبعة في وجود الصوديوم هيدروكسيد كعامل مساعد. كلا التفاعلين تم بواسطة الطحن في عدم وجود المذيبات كواحدة من طرق الكيمياء الخضراء في تقليل مخاطر المخلفات الكيميائية علي البيئة ، حيث اثبتت هذه الطريقة فعاليتها في اعطاء نسب عالية من النواتج. تم التأكد من البنية التركيبية للمركبات عن طريق مطياف الاشعة تحت الحمراء، التحليل الطيفي للاشعة فوق البنفسجية، كروماتوغرافيا الطبقة الرقيقة و درجة الانصهار.

## Contents

Title	Page
الآية	I
Dedication	II
Acknowledgement	III
Abbreviations	IV
Abstract	V
الخلاصة	VI
Contents	VII - VIII
list of Table	IX
list of Figure	X - XII
list of Scheme	XIII
1. Introduction	1
1.1 Computational Chemistry	1
1.2 Computational Tool	2
1.3 Quantitative Structure Activity Relationships	3
1.4 Molecular Docking	4
1.5 Solvent Free method	4
1.6 Enone ( $\alpha$ , $\beta$ –carbonyl) compounds	5
1.7 Pyrazolines	5
1.7.1 Structure of pyrazolines	5
1.7.2 Synthesis of Pyrazolines	6
1.8 Aim and objectives	8
2. Materials and Methods	9
2.1 Materials	9
2.1.1 Chemicals	9
2.1.2 Instruments	9
2.1.3 Apparatus	9
2.1.4 Thin layer chromatography (TLC)	9
2.1.5 Software Programmers	9
2.1.5.1 ACD lab/chemsketch	9
2.1.5.2 Moe 2009.10	10
2.1.5.3 Minitab 17	10
2.2 Methods	10
2.2.1 Modeling	10
2.2.2 Quantitative Structure Activity Relationships Experimental	13
2.2.2.1 Data set	13
2.2.2.2 Multi Linear Regression analysis (MLR)	13
2.2.3 Docking	15
2.2.3.1 Protein preparation	15
2.2.3.2 Preparation of the ligand	15
2.2.4 General Synthetic methods	15
2.2.4.1 enone synthesis (step1)	15
2.2.4.2 Pyrazoline synthesis (step2)	15
3 Results and Discussion	20
3.1 Quantitative structure reactivity relationship	20



3.1.1 Fit regression model	20
3.1.2 Validation of the model	20
3.2 Docking output	26
3.3 Synthesis of Pyrazoline compounds	28
3.3.1 Retro synthetic analysis (RSA)	30
3.3.2 Mechanism	30
3.3.2.1 Mechanism of Enone synthesis	30
3.3.2.2 Mechanism of Pyrazoline synthesis	31
3.3.3 Characterizations of the compounds	32
3.3.3.1 Thin layer chromatography	35
3.3.3.2 Ultra Violet/Visible spectroscopy	36
3.3.3.3 Infra-red	36
Conclusion	37
Recommendations	37
References	38
Appandix	40-65

## List of tables

Table (2.1) Designed pyrazoline compounds descriptors	11
Table (2.2) Observed PIC <sub>50</sub> for AsPC-1 and U251 cell line	14
Table (2.3) chemical name of the synthesized enone compounds:	18
Table(2.4)Chemical Name of the synthesized Pyrazoline Compounds	19
Table (3.1) validation models	20
Table (3.2) Predictive value (PIC <sub>50</sub> ) of the data set through QSAR model ...	22
Table (3.3) Predicated biological activity for the designed pyrazoline compounds	24
Table (3.4) Output of the Interaction between the ligand with5kk5 protein active sides	26
Table (3.5) Output of the Interaction of the ligand with 1NQU proteine active side	27
Table (3.6) Reaction conditions of synthesized enone compounds	28
Table (3.7) Reaction conditions of pyrazolines compounds	29
Table (3.8) Physical parameters of synthesized enone compounds	32
Table (3.9) Physical parameters of synthesized Pyrazolines	33
Table (3.10) The IR spectrum data of enone compounds	34
Table (3.11) The IR spectrum data of synthesized Pyrazolines	35

## *List of Figure*

Figure (1.1) Prazoline Structure	6
Figure (1.2) Tautomeric Structure of Pyrazoline	6
Figure (3.1) Predicted pancreatic anticancer activities by (MLR) in comparison with experimental values	23
Figure (3.2) Predicted glioblastoma anticancer activities by (MLR) in comparison with experimental values	23
Figure (3.3) The interactions between the ligand (compound VIII) and the 5kk5 protein active side	40
Figure (3.4) The interactions between the ligand (compound IX) and the 5kk5 protein active side	40
Figure (3.5) The interactions between the ligand (compound X) and the 5kk5 protein active side	40
Figure (3.6) The interactions between the ligand (compound XI) and the 5kk5 protein active side	41
Figure (3.7) The interactions between the ligand (compound XII) and the 5kk5 protein active side	41
Figure (3.8) The interactions between the ligand (compound XIII) and the 5kk5 protein active side	41
Figure (3.9) The interactions between the ligand (compound XIV) and the 5kk5 protein active side	42
Figure (3.10) The interactions between the ligand (compound XV) and the 5kk5 protein active side	42
Figure (3.11) The interactions between the ligand (compound XVI) and the 5kk5 protein active side	42
Figure (3.12) The interactions between the ligand (compound XVII) and the 5kk5 protein active side	43
Figure (3.13) The interactions between the ligand (compound XVIII) and the 5kk5 protein active side	43
Figure (3.14) The interactions between the ligand (compound XIX) and the 5kk5 protein active side	43
Figure (3.15) The interactions between the ligand (compound XX) and the 5kk5 protein active side	44
Figure (3.16) The interactions between the ligand (compound XXI) and the 5kk5 protein active side	44
Figure (3.17) The interactions between the ligand (compound XXII) and the 5kk5 protein active side	44
Figure (3.18) The interactions between the ligand (compound XXIII) and the 5kk5 protein active side	45
Figure (3.19) The interactions between the ligand (compound XXIV) and the 5kk5 protein active side	45
Figure (3.20) The interactions between the ligand (compound XXV) and the 5kk5 protein active side	45
Figure (3.21) The interactions between the ligand (compound XXVI) and the 5kk5 protein active side	46
Figure (3.22) The interactions between the ligand (compound XXVII) and the 5kk5 protein active side	46
Figure (3.23) The interactions between the ligand (compound XXVIII) and the	46

5kk5 protein active side	
Figure (3.24) The interactions between the ligand (compound XXIX) and the 5kk5 protein active side	47
Figure (3.25) The interactions between the ligand (compound XXX) and the 5kk5 protein active side	47
Figure (3.26) The interactions between the ligand (compound XXXI) and the 5kk5 protein active side	47
Figure (3.27) The interactions between the ligand (compound XXXII) and the 5kk5 protein active side	48
Figure (3.28) The interactions between the ligand (compound XXXIII) and the 5kk5 protein active side	48
Figure (3.29) The interactions between the ligand (compound XXXIV) and the 5kk5 protein active side	48
Figure (3.30) The interactions between the ligand (compound XXXV) and the 5kk5 protein active side	49
Figure (3.31) The interactions between the ligand (compound VIII) and the 1NQU protein active side	49
Figure (3.32) The interactions between the ligand (compound IX) and the 1NQU protein active side	49
Figure (3.33) The interactions between the ligand (compound X) and the 1NQU protein active side	50
Figure (3.34) The interactions between the ligand (compound XI) and the 1NQU protein active side	50
Figure (3.35) The interactions between the ligand (compound XII) and the 1NQU protein active side	50
Figure (3.36) The interactions between the ligand (compound XIII) and the 1NQU protein active side	51
Figure (3.37) The interactions between the ligand (compound XIV) and the 1NQU protein active side	51
Figure (3.38) The interactions between the ligand (compound XV) and the 1NQU protein active side	51
Figure (3.39) The interactions between the ligand (compound XVI) and the 1NQU protein active side	52
Figure (3.40) The interactions between the ligand (compound XVII) and the 1NQU protein active side	52
Figure (3.41) The interactions between the ligand (compound XVIII) and the 1NQU protein active side	52
Figure (3.42) The interactions between the ligand (compound XIX) and the 1NQU protein active side	53
Figure (3.43) The interactions between the ligand (compound XX) and the 1NQU protein active side	53
Figure (3.44) The interactions between the ligand (compound XXI) and the 1NQU protein active side	53
Figure (3.45) The interactions between the ligand (compound XXII) and the 1NQU protein active side	54
Figure (3.46) The interactions between the ligand (compound XXIII) and the 1NQU protein active side	54
Figure (3.47) The interactions between the ligand (compound XXIV) and the 1NQU protein active side	54

Figure (3.48) The interactions between the ligand (compound XXV) and the 1NQU protein active side	55
Figure (3.49) The interactions between the ligand (compound XXVI) and the 1NQU protein active side	55
Figure (3.50) The interactions between the ligand (compound XXVII) and the 1NQU protein active side	55
Figure (3.51) The interactions between the ligand (compound XXVIII) and the 1NQU protein active side	56
Figure (3.52) The interactions between the ligand (compound XXIX) and the 1NQU protein active side	56
Figure (3.53) The interactions between the ligand (compound XXX) and the 1NQU protein active side	56
Figure (3.54) The interactions between the ligand (compound XXXI) and the 1NQU protein active side	57
Figure (3.55) The interactions between the ligand (compound XXXII) and the 1NQU protein active side	57
Figure (3.56) The interactions between the ligand (compound XXXIII) and the 1NQU protein active side	57
Figure (3.57) The interactions between the ligand (compound XXXIV) and the 1NQU protein active side	58
Figure (3.58) The interactions between the ligand (compound XXXV) and the 1NQU protein active side	58
Figure (3.59) The IR spectrum of compound I	59
Figure (3.60) The IR spectrum of compound II	59
Figure (3.61) The IR spectrum of compound III	60
Figure (3.62) The IR spectrum of compound IV	60
Figure (3.63) The IR spectrum of compound V	61
Figure (3.64) The IR spectrum of compound VI	61
Figure (3.65) The IR spectrum of compound VII	62
Figure (3.66) The IR spectrum of compound VIII	62
Figure (3.67) The IR spectrum of compound IX	63
Figure (3.68) The IR spectrum of compound X	63
Figure (3.69) The IR spectrum of compound XI	64
Figure (3.70) The IR spectrum of compound XII	64
Figure (3.71) The IR spectrum of compound XIII	65
Figure (3.72) The IR spectrum of compound XIV	65

### *List of Scheme*

Scheme (2.1) synthesis of the pyrazoline compounds via p-nitro acetophenone precursor	16
Scheme (2.2) synthesis of the pyrazoline compounds via acetone precursor	17
Scheme (3.1) Pyrazoline retro synthetic analysis	30
Scheme (3.2) Claisen-Schmidt condensation mechanism	30
Scheme (3.3) Pyrazoline synthesis mechanism	31

# **Chapter One**

## **1. Introduction**

## 1.1 Computational Chemistry:

The term theoretical chemistry may be defined as the mathematical description of chemistry. The term computational chemistry is generally used when a mathematical method is sufficiently well developed that it can be automated for implementation on a computer. Note that the words "exact" and "perfect" do not appear in these definitions. Very few aspects of chemistry can be computed exactly, but almost every aspect of chemistry has been described in a qualitative or approximately quantitative computational scheme. The biggest mistake a computational chemist can make is to assume that any computed number is exact. However, just as not all spectra are perfectly resolved, often a qualitative or approximate computation can give useful insight into chemistry if the researcher understands what it does and does not predict (Young, D.C. 2001).

Computational chemistry (also called molecular modeling; the two terms mean about the same thing) is a set of techniques for investigating chemical problems on a computer. Questions commonly investigated computationally are:

Molecular geometry: the shapes of molecules – bond lengths, angles and dihedrals. Energies of molecules and transition states: this tells us which isomer is favored at equilibrium, and (from transition state and reactant energies) how fast a reaction should go. Chemical reactivity: for example, knowing where the electrons are concentrated (nucleophilic sites) and where they want to go (electrophilic sites) enables us to predict where various kinds of reagents will attack a molecule.

IR, UV and NMR spectra: these can be calculated, and if the molecule is unknown, someone trying to make it knows what to look for.

The interaction of a substrate with an enzyme: Seeing how a molecule fits into the active site of an enzyme is one approach to designing better drugs.

The physical properties of substances: These depend on the properties of individual molecules and on how the molecules interact in the bulk material. For example, the strength and melting point of a polymer (e.g. a plastic) depend on how well the molecules fit together and on how strong the forces between them are (Lewars, E. 2004).



## 1.2 Computational Tool:

The main tools available belong to five broad classes as described below:

1. Molecular mechanics (MM) is based on a model of a molecule as a collection of balls (atoms) held together by springs (bonds). By known of the normal spring lengths and the angles between them, and how much energy it takes to stretch and bend the springs, the energy can be calculated of a given collection of balls and springs, i.e. of a given molecule; changing the geometry until the lowest energy is found enables us to do a geometry optimization, i.e. to calculate a geometry for the molecule. Molecular mechanics is fast: a fairly large molecule can be optimized in seconds on a powerful desktop computer (a workstation); on a personal computer the job might also take only a few seconds.
2. Ab initio calculations (is from the Latin: “from first principles”) are based on the Schrodinger equation. This is one of the fundamental equations of modern physics and describes, among other things, how the electrons in a molecule behave. The ab initio method solves the Schrodinger equation for a molecule and gives us the molecule’s energy and wavefunction. The wavefunction is a mathematical function that can be used to calculate the electron distribution (and, in theory at least, anything else about the molecule). From the electron distribution we can tell things like how polar the molecule is, and which parts of it are likely to be attacked by nucleophiles or electrophiles.
3. Semi empirical (SE) calculations are, like ab initio, based on the Schrodinger equation.
4. Density functional calculations (often called density functional theory (DFT) calculations) are, like ab initio and SE calculations, based on the Schrodinger equation. However, unlike the other two methods, DFT does not calculate a wavefunction, but rather derives the electron distribution (electron density function) directly. A functional is a mathematical entity related to a function.
5. Molecular dynamics calculations apply the laws of motion to molecules. Thus one can simulate the motion of an enzyme as it changes shape on binding to a substrate, or the motion of a swarm of water molecules around a molecule of solute (Lewars, E. 2004).

At one time, computational chemistry techniques were used only by experts extremely experienced in using tools that were for the most part difficult to understand and apply. Today, advances in software have produced programs that are easily used by any chemist. Along with new software comes new literature on the subject. There are now books that describe the fundamental principles of computational chemistry at almost any level of detail. A number of

books also exist that explain how to apply computational chemistry techniques to simple calculations appropriate for student assignments. There are, in addition, many detailed research papers on advanced topics that are intended to be read only by professional theorists (Lewars, E. 2004).

### **1.3 Quantitative Structure Activity Relationships (QSAR):**

To search for the existence of any correlation among different objects or observation is a natural human tendency. Structure activity relationship (QSAR) modeling was evolved from the idea of possible existence of a mathematical correlation between the nature of a chemicals and their behavioral manifestation. Following the initial observation, the "chemical nature" was conceptualized and explored in terms of information extractable from the structure and property of chemicals.

Properties elicited by chemicals are significantly influenced by the nature of their chemical structure (branching, functional groups, electronegative behavior, stereo chemical features, etc.), as well as different physicochemical properties (hydrophobicity, electronic nature, steric influence, etc.). The development of suitable descriptors (predictor variables) possessing a potential diagnostic nature in extracting the chemical attributes can help in exploring the mechanistic basis involved in a chemical biological process following mathematical model development. Thus, QSAR studies allow a rational explanation for the behavioral manifestation of chemicals accompanied with providing knowledge on the mechanism involved, thereby creating an opportunity to tune the behavior of a chemical. As it provides a good alternative method to laboratory experimentation, at least for initial screening, QSAR is utilized in costly research like the design drug molecules and assessment of chemical hazards (Roy, K.; *etal* 2015).

Quantitative structure activity relationship (QSAR) is one of the most widely used tools to design newer candidates for several therapeutic areas. It provides useful insights into the structural features which are responsible for the biological activity and help to generate a mathematical model which can predict activity of untested compounds quantitatively. QSAR study usually leads to a predictive formula by correlation of physicochemical properties of a congeneric series with the biological activity (Soni, H., *et al* 2015).

#### **1.4 Molecular Docking:**

Molecular docking has become an increasingly important tool in drug discovery. The molecular docking also can be used to model the interaction between a small molecule and a protein at the atomic level. This which allows us to characterize the behavior of small molecules in the binding site of target proteins as well as to elucidate fundamental biochemical processes (Jasril, J. *et al* 2017).

#### **1.5 Solvent Free method:**

Though it is a common practice to run the organic reactions in solvent media, the chemists' concern to minimize the environmental pollution caused by solvents and also their academic interest in solid-solid reactions have led them in recent times to develop methodologies for solvent free reactions with considerable success.

A general assumption with regard to organic reactions is that they are performed in a solvent medium. The rationale behind this concept is simple. That is, the reactants can interact effectively if they are in a homogeneous solution, which facilitates the stirring, shaking or other ways of agitation, where by the reactant molecules come together rapidly and continuously. A solvent-free or solid state reaction may be carried out using the reactants alone or incorporating them in clays, zeolites, silica, alumina or other matrices.

Thermal process or irradiation with UV, microwave or ultrasound can be employed to bring about the reaction. Solvent-free reactions obviously reduce pollution, and bring down handling costs due to simplification of experimental procedure, work up technique and saving in laboratory. These would be especially important during industrial production. Often, the products of solid state reactions turn out to be different from those obtained in solution phase reactions. This is because of specific spatial orientation or packing of the reacting molecules in the crystalline state. This is true not only of the crystals of single compounds, but also of co-crystallized solids of two or even more reactant molecules. The host-guest interaction complexes obtained by simply mixing the components intimately also adopt ordered structure. The orientation requirements of the substrate molecules in the crystalline state have provided excellent opportunities to achieve high degree of stereo selectivity in the products. This has made it possible to synthesize chiral molecules from prochiral ones either by complexation with chiral hosts or formation of intermediates with chiral partners (Nagendrappa, G. 2002).

## 1.6 Enone ( $\alpha$ , $\beta$ –carbonyl) compounds:

$\alpha$ ,  $\beta$ -unsaturated enones are important intermediates in many addition reactions of nucleophiles due to inductive polarization of carbonyl group at the  $\beta$ -position. Several strategies for the synthesis of these systems based on the formation of carbon-carbon bond have been reported, and among them the direct aldol condensation and Claisen-Schmidt condensation still occupy prominent positions (Bora, *et al* 2005).

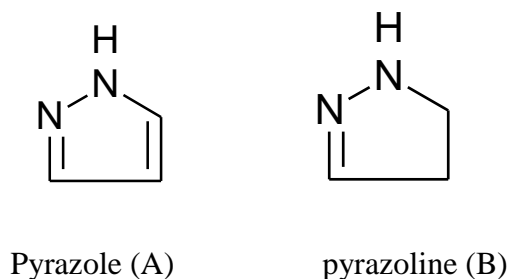
## 1.7 Pyrazolines:

$\alpha,\beta$  -Unsaturated ketones constitute an important class of naturally occurring flavonoid compounds that exhibit a wide spectrum of biological activities such as anticancer, anti-inflammatory, antiviral and antibacterial activities etc. These are well-known intermediates for the synthesis of a large number of bioactive molecules, such as pyrazolines, pyrimidines, isoxazolines and thiazolines.

Amongst nitrogen containing five membered hetero cycles, pyrazolines have proved to be the most useful framework for biological activities. The dihydropyrazoles are called pyrazolines. Pyrazolines have attracted attention of medicinal chemists for both with regard to heterocyclic chemistry and the pharmacological activities associated with them and various methods have been carried out for their synthesis. Considerable attention has been focused on pyrazolines and substituted pyrazolines due to their interesting biological activities. The pharmaceutical importance of these compounds lies in the fact that they can be effectively utilized as antibacterial, antifungal, antiviral, antiparasitic, antitubercular, herbicidal, fungicidal, analgesic, antioxidant, antipyretic, insecticidal, anticancer, antitumor, antidiabetic, anticonvulsant, antidepressant and anti-inflammatory agents. Moreover, many selectively fluoro-substituted pyrazolines show promising agrochemical properties (Jayaroopa, P. 2013).

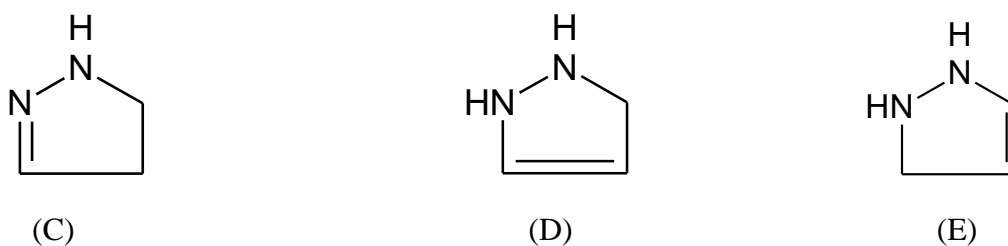
### 1.7.1 Structure of pyrazolines:

A five membered ring containing adjacent nitrogen atoms was termed as pyrazole (A) by Knorr in 1883. The dihydropyrazole is called as pyrazoline (B)(figure 1.1).



**Figure (1.1) Pyrazoline Structure**

If the nitrogen atom in pyrazoline is substituted, tautomerism is exhibited by the structures C, D and E. The tautomers C and D are more stable than E and are known as  $\Delta^2$ -pyrazolines and  $\Delta^3$ -pyrazolines respectively. No evidence for the stability of tautomer E has been reported (Junghare, N. 2001).



**Figure (1.2) Tautomeric Structure of Pyrazoline**

### 1.7.2 Synthesis of Pyrazolines:

The most convenient method for the synthesis of pyrazoline is the action of hydrazine hydrate or hydrazine derivatives on  $\alpha$ ,  $\beta$ -carbonyl compounds. The intermediate formed is a hydrazone or phenylhydrazone respectively. This was subsequently cyclised to pyrazoline, in the presence of a suitable cyclizing reagent.

The most widely used reagent for cyclization of hydrazone is acetic acid/ Alcohol containing a little HCl also serves this purpose, but gives poor yield. The rate of cyclization of hydrazone to pyrazoline also depends upon the nature of R. It is in the order  $R=\text{Ph}>\text{Me}>\text{H}$  (Junghare, N. 2001).

The mechanism of the formation of pyrazoline was suggested by Aubagnac et al" From  $\alpha$ ,  $\beta$ -unsaturated ketones by 1, 4 addition of phenyl hydrazine through an adduct intermediate. The rate determining step is the dehydration giving hydrazone which has been supported from the activation energy calculation of 1, 3, 5-tripyrzoline. The cyclization of pyrazoline is shown to be spontaneous (Junghare, N. 2001).

### **1.8 Aim and objectives:**

- Modeling some of 3, 5 di-substituted pyrazoline derivatives using ACD lab program.
- To develop QSAR model to predict the biological activity of the modeling pyrazoline derivatives as potent AsPC-1 human pancreatic cell line and U251 human glioblastoma cell lines.
- To elucidate the interaction between the inhibitor molecules through molecular docking.
- To prepare seven compounds of some of 3, 5 di-substituted pyrazoline derivatives under solvent-free condition (grinding technique).

# **Chapter Two**

## **2. Materials and Methods**



## **2.1 Materials:**

### **2.1.1 Chemicals:**

N, N DimethylaminoBenzaldehyde, Acetaldehyde Assay (20-30%) ALPH CHEMIKA India, P-BromoBenzaldehyde, Benzaldehyde Minimum Assay 98% LOBA Chemica India, P-nitro Acetophenone Assay G.C (min 98%) LOBA Chemie India, Acetone 99% Assay (GC) (min 99%) LOBA Chemie, Sodium hydroxide Assay (95.0-100.5%) J.T Baker Sweden, Hydrazine sulphate Alpha chemika India, Ethyl alcohol Assay (94.8-95.8 vol %) REAGENT DUKSAN.

### **2.1.2 Instruments:**

IR300, Spectrometer (Thermo Nicolet), 7205 UV/Visible Spectrophotometer (JENWAY), Melting Point.

### **2.1.3 Apparatus:**

A mortar, pestle, spatula, beakers 50ml, glass rod and funnel, (all glass ware were Pyrex type).

### **2.1.4 Thin layer chromatography (TLC):**

Thin layer chromatography was carried out using pre-coated LK5DF silica gel from Whatman Inc, by using n-hexane and ethyl acetate (1:3) as mobile phase.

### **2.1.5 Programs software:**

- **2.1.5.1** ACD lab/chemsketch free ware 2015 downloaded from [www.acd-labs.com](http://www.acd-labs.com):

ChemSketch (we tested free ware 2015) is a graphic interface that can be used as the front end for a host of programs sold by Advanced Chemistry Development.

Both free and commercial versions are available. It is a two-dimensional structure drawing program primarily designed for organic molecules. Although the drawing mode is essentially a two-dimensional drawing routine, it is also possible to rotate the molecule in three dimensions. The program automatically keeps track of the number of hydrogens bonded to each atom. The reviewer felt that the molecule sketch mode was convenient to use.

- **2.1.5.2 Moe 2009.10:**

MOE (Version 2009.02) stands for molecular operating environment. The developers of this package took the unique approach of creating a programming language for writing molecular modeling software. The package currently includes molecular mechanics, dynamics, periodic boundary conditions, QSAR, a combinatorial builder, and many functions ideal for protein modeling, including multiple-sequence alignment and homology model building. Functions are also available for computing polymer properties and direction patterns. Several conformation search routines are included. Other property calculations include log P and molar refractivity calculation. The graphic interface is a multitasking environment that works well. The protein and carbohydrate builders are particularly convenient to use. The small-molecule builder has a selection of common organic functional groups as well as individual atoms for organics and common hetero atoms. There are a number of rendering modes to create fairly nice graphic images. However, the program does not have a way to save the display as an image file. MOE can be accessed through a Web browser also.

- **2.1.5.3 Minitab 17:**

Throughout Getting Started with Minitab 17, you analyze data from the shipping centers as you learn to use Minitab.

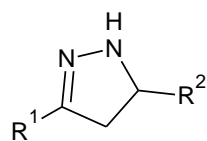
You create graphs and perform statistical analyses to identify the shipping center that has the most efficient computer system. You then concentrate on the data from this shipping center. First, you create control charts to test whether the shipping center's process is in control. Then, you perform a capability analysis to test whether the process is operating within specification limits. Finally, you perform a designed experiment to determine ways to improve those processes.

## **2.2 Methods:**

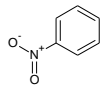
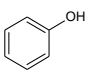
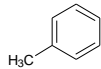
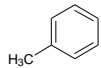
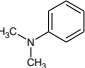
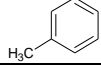
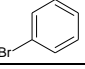
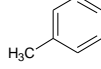
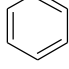
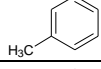
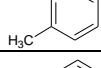
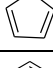
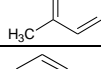
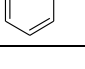
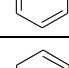
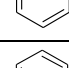
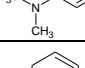
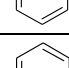
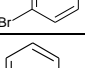
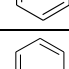
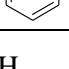
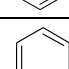
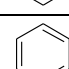
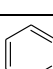
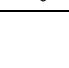
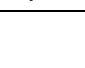
### **2.2.1 Modeling:**

28Pyrzoline derivative compounds were modeled by using two-dimensional structure drawing mode (table 2.1). Then some of their properties were generated by using ACD lab and MOE 2009 software.

**Table (2.1) Designed Pyrazoline compounds descriptors**



N.O	R <sup>1</sup>	R <sup>2</sup>	M.F	F.Wt	S log P	S log_VSA4	AM1_di pole	AM1_H OMO
VIII		CH <sub>3</sub>	C <sub>10</sub> H <sub>11</sub> N <sub>3</sub> O <sub>2</sub>	205.213	1.6807	3.1856	6.7783	- 9.2473
IX			C <sub>17</sub> H <sub>18</sub> N <sub>4</sub> O <sub>2</sub>	310.350	3.195	6.3712	8.1496	- 8.4847
X			C <sub>15</sub> H <sub>12</sub> BrN <sub>3</sub> O <sub>2</sub>	346.178	3.8915	6.3712	5.5877	- 9.4216
XI			C <sub>15</sub> H <sub>13</sub> N <sub>3</sub> O <sub>2</sub>	267.282	3.1290	6.3712	6.6009	- 9.2872
XII	CH <sub>3</sub>		C <sub>12</sub> H <sub>17</sub> N <sub>3</sub>	203.283	2.9549	3.1856	2.8672	- 9.2779
XIII	CH <sub>3</sub>		C <sub>10</sub> H <sub>11</sub> BrN <sub>2</sub>	239.111	2.2584	3.1856	2.5694	- 8.2653
XIV	CH <sub>3</sub>		C <sub>10</sub> H <sub>12</sub> N <sub>2</sub>	160.215	23.861	3.1856	2.4444	- 9.1275
XV	CH <sub>3</sub>	CH <sub>3</sub>	C <sub>5</sub> H <sub>10</sub> N <sub>2</sub>	98.146	0.7441	0.0000	2.6843	-9.0872
XVI	CH <sub>3</sub>	H	C <sub>4</sub> H <sub>8</sub> N <sub>2</sub>	84.120	0.3556	0.0000	2.7302	-9.1239
XVII	CH <sub>3</sub>		C <sub>8</sub> H <sub>10</sub> N <sub>2</sub> O	150.178	1.7854	5.4488	2.1379	-9.1515
XVIII	CH <sub>3</sub>		C <sub>10</sub> H <sub>12</sub> N <sub>2</sub> O	176.215	1.8980	3.1856	2.8382	-9.0732
XIX		H	C <sub>9</sub> H <sub>9</sub> N <sub>3</sub> O <sub>2</sub>	191.187	1.2922	3.1856	6.5800	-9.3003
XX			C <sub>13</sub> H <sub>11</sub> N <sub>2</sub> O <sub>3</sub>	257.245	2.7220	8.6344	6.385	-9.4031

N.O	R <sup>1</sup>	R <sup>2</sup>	M.F	F.Wt	S log P	S log_VSA4	AM1_dipole	AM1_HOMO
XXI			C <sub>15</sub> H <sub>13</sub> N <sub>3</sub> O <sub>3</sub>	283.282	2.8346	6.3712	6.2701	-9.2432
XXII		CH <sub>3</sub>	C <sub>11</sub> H <sub>14</sub> N <sub>2</sub>	174.242	2.0809	6.3712	2.3963	-8.5856
XXIII			C <sub>18</sub> H <sub>21</sub> N <sub>3</sub>	279.379	3.5952	9.5567	2.3023	-8.2778
XXIV			C <sub>10</sub> H <sub>15</sub> BrN <sub>2</sub>	315.208	4.2917	9.5567	2.8346	-8.7457
XXV			C <sub>16</sub> H <sub>16</sub> N <sub>2</sub>	236.312	3.5292	9.5567	2.2942	-8.6446
XXVI		H	C <sub>10</sub> H <sub>12</sub> N <sub>2</sub>	160.216	1.6924	6.3712	2.4503	-8.6206
XXVII			C <sub>14</sub> H <sub>14</sub> N <sub>2</sub> O	226.274	3.1222	11.8200	1.9828	-8.7375
XXVIII			C <sub>16</sub> H <sub>16</sub> N <sub>2</sub> O	253.311	3.2348	9.5567	2.7362	-8.8869
XXIX		CH <sub>3</sub>	C <sub>10</sub> H <sub>12</sub> N <sub>2</sub>	160.216	1.7725	3.1856	2.4071	-8.6969
XXX			C <sub>17</sub> H <sub>19</sub> N <sub>3</sub>	265.353	3.2868	6.3712	2.4817	-8.3047
XXXI			C <sub>15</sub> H <sub>11</sub> BrN <sub>2</sub>	299.165	4.0462	6.3712	4.0419	-8.9773
XXXII			C <sub>15</sub> H <sub>14</sub> N <sub>2</sub>	222.285	3.2208	6.3712	2.2687	-8.7610
XXXIII		H	C <sub>9</sub> H <sub>10</sub> N <sub>2</sub>	146.189	1.3840	3.1856	2.4662	-8.7379
XXXIV			C <sub>13</sub> H <sub>12</sub> N <sub>2</sub> O	212.247	2.8138	8.6344	2.7008	-8.8708
XXXV			C <sub>15</sub> H <sub>14</sub> N <sub>2</sub> O	238.284	2.9264	6.3712	2.6659	-8.9742

- M.F and F.wt were calculated using ACD lab.
- Slog p, Slog\_VSA4, AM1\_dipole and AM1\_Homo were calculated using MOE2009.

## 2.2.2 Quantitative Structure Activity Relationship Experimental:

### 2.2.2.1 Data set:

From literature (e.i. Karabacak, M. *etal* 2015) twelve compounds of 3, 5 di-substituted pyrazoline derivatives reported and evaluated for their biological activity effects as potential anticancer agents against AsPC-1 human pancreatic and U251 human glioblastoma cell lines respectively was selected. The twelve compounds were randomly divided into ten compounds as a training set and two compounds as test set. Structures of all the compounds were used for 2D-QSAR analysis and their anticancer activity ( $IC_{50}$  mM) are given in Table (2.2). For all these compounds, the values of biological activity ( $IC_{50}$   $\mu$ M) were converted to (mM) then they were used in the negative logarithmic scale ( $PIC_{50}$ ) to achieve normal distribution. Structures of all compounds were sketched by ACD Lab and then some descriptors were calculated using ACD/lab and MOE2009 software.

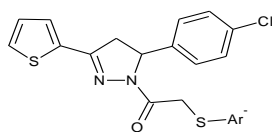
### 2.2.2.2 Multi Linear Regression Analysis (MLR):

It is a statistic technique used to study the relation between one dependent variable and several independent variables to minimize the differences between actual and predicted values (Samira, M.; *etal*, 2011).

Minitab 17 software was used to check the correlation between the dependent variables ( $PCI_{50}$ ) and the independent variables (descriptors) and also to check the inter-correlation between the descriptors themselves which have a correlated with the dependent variable to avoid the multicollinearity. Eight descriptors were calculated by ACD lab (Formula weight, Molar refractivity, Molar volume, Index of refraction, Surface tension, Density, Polarizability and log P) plus twenty two descriptors (energy, slog p, slog p\_VSA0, slog p\_VSA1 ..... slog p\_VSA9, SMR\_VSA0, SMR\_VSA1, SMR\_VSA2 ..... SMR\_VSA6 and SMR\_VSA7) were calculated by MOE2009.1. Then were subjected to correlation analysis to generate MLR for model (1). Beside this another four descriptors (AM1\_dipole, AM1\_Homo, AM1\_lumo and ASA\_H) were calculated by Moe 2009.01 to generate MLR for model (2)

Inter data >> stat >> basic statistics >> correlation.

**Table (2.2) Observed PIC<sub>50</sub> for AsPC-1 and U251 cell line**



	Compound N.O	Ar	Observed PIC <sub>50</sub> mM	
			AsPC-1 cell line	U251 cell line
Training set	1		0.301029996	0.30103
	2		0.301029996	0.30103
	3		1.187086643	0.30103
	4		0.666149855	0.30103
	5		0.700492701	0.30103
	6		0.626720107	0.30103
	7		0.856048884	0.4055
	8		0.966174306	0.30103
	9		0.956637722	0.77833
	10		1.774690718	1.92445
Test set	11		0.945	0.88639
	12		1.207	0.1.15428

### **2.2.3 Docking:**

#### **2.2.3.1 Protein preparation:**

Molecular docking was conducted using MOE 2009.10 software. The (5kk5) human pancreatic and (1NQU) human glioblastoma (brain cancer) protein inhibitors structures were downloaded from the protein data bank and they were used as the macromolecules for molecular docking. These proteins were kept in rigid, for then, all hydrogen atoms were added.

#### **2.2.3.2 Preparation of the ligand:**

The Pyrazoline derivatives which were designed (table 2.1) were used as the ligands and drawn using ACD/Lab software. These ligands were required to minimize the energies for then the minimized structures were subsequently prepared with the detected root of torsion and number of torsions for flexible-ligand docking using MOE 2009.10 software.

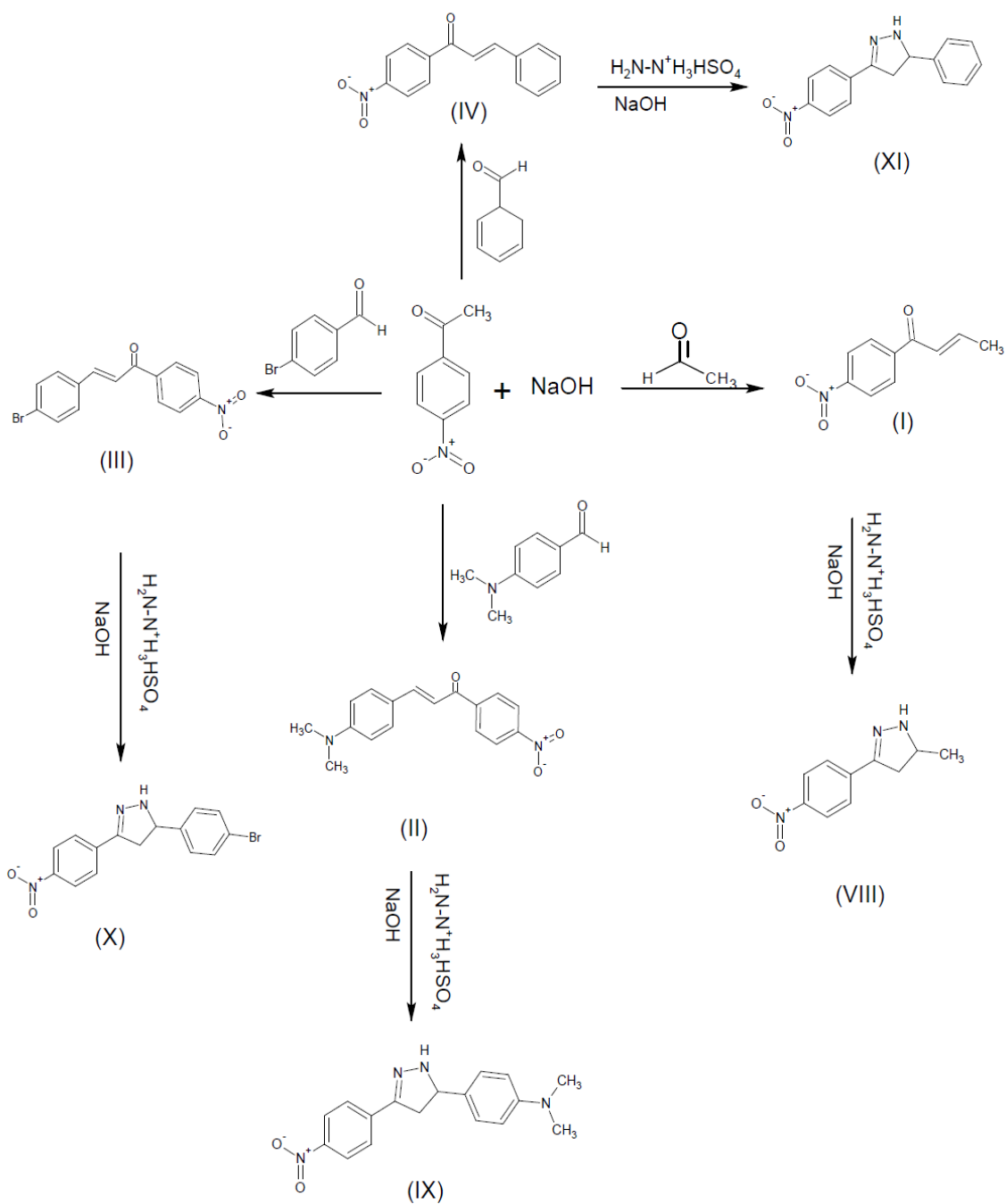
### **2.2.4 General Synthetic Methods:**

#### **2.2.4.1 Enone Synthesis (step1):**

(2.5m mole) of the required ketone with (2.5m mole) of the required aldehyde and (0.1g, 2.5m mole) of sodium hydroxide were weighted and then transferred to the mortar and grinded by a pistol at room temperature until the desired product was obtained. Then the product was transferred by water to beaker (50ml) and was kept for 24 hours. After that it was filtered and the percentage yield was calculated. The solid formed was recrystallized with ethanol (95%).

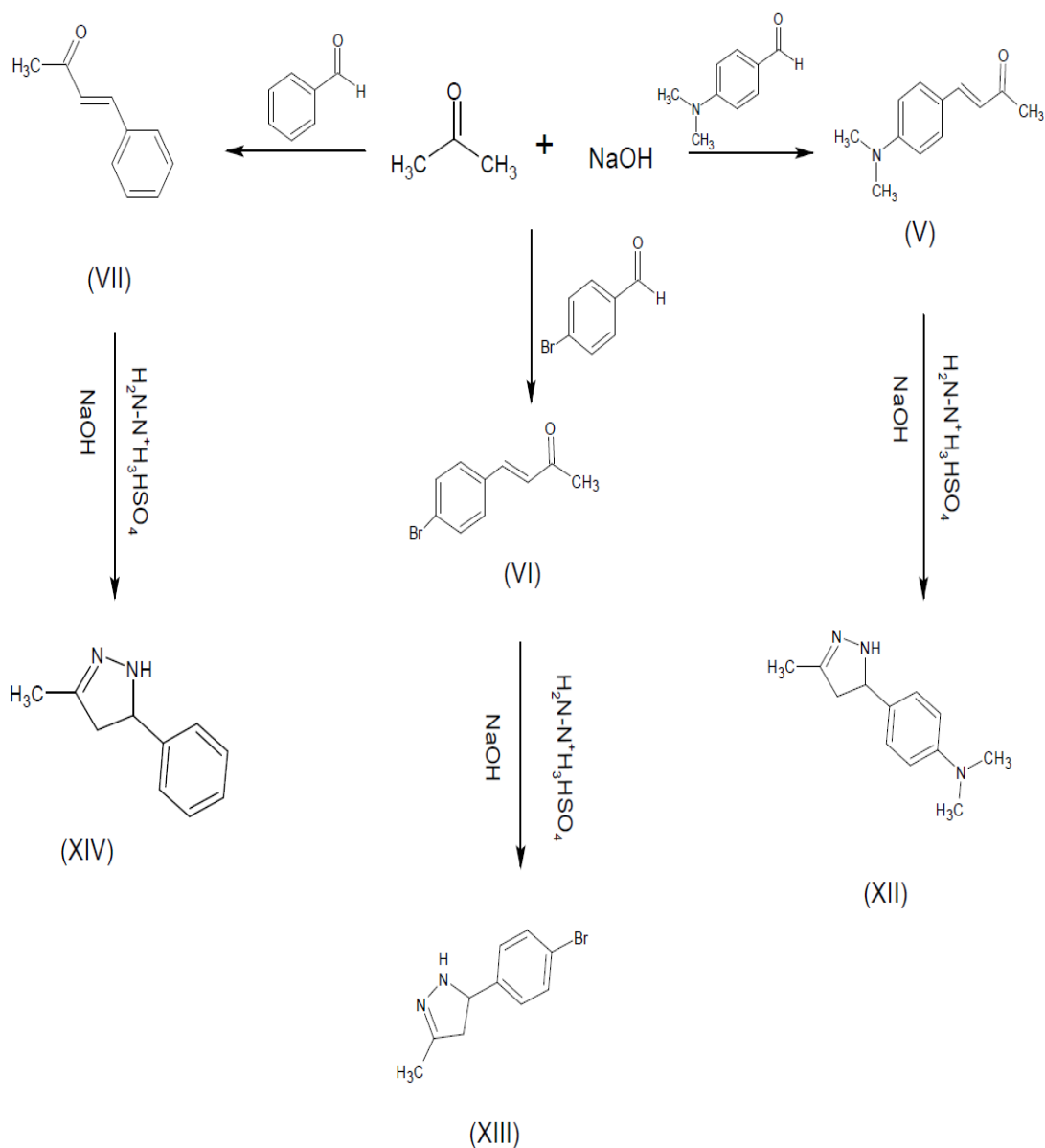
#### **2.6.4.2 Pyrazoline Synthesis (step2):**

(1.25m mole) of the required enone (which prepared in step 1), with (0.163g, 1.25m mole) of hydrazine sulphate and (0.05g, 1.25m mole) of sodium hydroxide were weighted and then transferred to the mortar and grinded by a pistol at room temperature until the desired product was obtained. Then the product was transferred by water to beaker (50ml) and was kept for 24 hours. After that it was filtered and the percentage yield was calculated. The solid formed was recrystallized with ethanol (95%).



**Scheme (2.1) synthesis of the pyrazoline compounds via p-nitro acetophenone as a precursor**

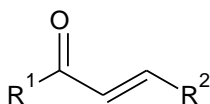




### Scheme (2.2) synthesis of the pyrazoline compounds via acetone as a precursor

The synthesis of new pyrazoline derivatives (VIII -XIV) was carried out according to the steps shown in Scheme (2.1 and 2.2). In the initial step,  $\alpha$ ,  $\beta$  unsaturated compounds (enone) was synthesized via the base-catalyzed Claisen-Schmidt condensation of p-nitro acetophenone and acetone with the required aldehyde, the ring closure reaction of the enone with hydrazine sulphate via the base-catalyzed afforded 3,5 di-substituted pyrazoline, all compounds obtained under solvent free condition methodology.

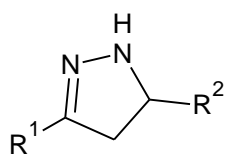
**Table (2.3) chemical name of the synthesized enone compounds:**



Compound N.O	R <sup>1</sup>	R <sup>2</sup>	Chemical Name
I		CH <sub>3</sub>	(2E)-1-(4-nitrophenyl)but-2-en-1-one
II			(2E)-3-[4-(dimethylamino)phenyl]-1-(4-nitrophenyl)prop-2-en-1-one
III			(2E)-3-(4-bromophenyl)-1-(4-nitrophenyl)prop-2-en-1-one
IV			(2E)-1-(4-nitrophenyl)-3-phenylprop-2-en-1-one
V	CH <sub>3</sub>		(3E)-4-[4-(dimethylamino)phenyl]but-3-en-2-one
VI	CH <sub>3</sub>		(3E)-4-(4-bromophenyl)but-3-en-2-one
VII	CH <sub>3</sub>		(3E)-4-phenylbut-3-en-2-one

- The chemical name was generated by using ACD/lab.

**Table (2.4) Chemical Name of the synthesized Pyrazoline Compounds:**



Compound NO.	R <sup>1</sup>	R <sup>2</sup>	Chemical Name
VIII		CH <sub>3</sub>	5-methyl-3-(4-nitrophenyl)-4,5-dihydro-1H-pyrazole
IX			N, N-dimethyl-4-[3-(4-nitrophenyl)-4,5-dihydro-1H-pyrazol-5-yl] aniline
X			5-(4-bromophenyl)-3-(4-nitrophenyl)-4,5-dihydro-1H-pyrazole
XI			3-(4-nitrophenyl)-5-phenyl-4,5-dihydro-1H-pyrazole
XII	CH <sub>3</sub>		N,N-dimethyl-4-(3-methyl-4,5-dihydro-1H-pyrazol-5-yl)aniline
XIII	CH <sub>3</sub>		5-(4-bromophenyl)-3-methyl-4,5-dihydro-1H-pyrazole/
XIV	CH <sub>3</sub>		3-methyl-5-phenyl-4,5-dihydro-1H-pyrazole

- The chemical name was generated by using ACD/lab.

# **Chapter Three**

## **3. Results and Discussion**

### 3.1 Quantitative Activity Relationship:

From the MLR analysis results found that:

The  $PCI_{50}$  has a correlated with (log p), formula weight and slogp\_VSA4. But also found that (log p) and (slog p) has a high correlated to each other so (slog p) was used instead of (log p) for AsPC-1 cell line data regression analysis. And  $PCI_{50}$  has a correlated with AM1\_dipole and AM1\_Humofor U251 cell line data regression analysis.

The statistical analysis or correlation analysis results based on the value of Pearson correlation (is a measure of the linear correlation between two variables X and Y, it has a value between +1 and -1, where 1 is total positive linear correlation, 0 is no linear correlation, and -1 is total negative linear correlation) and the P-value.

#### 3.1.1 Fit regression model:

Minitab 17 software was used to generate the fit regression model (Stat >> regression >> regression >> fit regression model).

The QSAR model (with three descriptors) built due to P  $IC_{50}$  value for AsPC-1 cell line using multiple linear regressions (MLR) method is represented by the following equation:

$$pCI_{50} = -3.16 + 0.046 \text{ slog P} + 0.00524 \text{ Formula weight} + 0.2629 \text{ Slog\_VSA4} \quad \text{model (1)}$$

The QSAR model (with two descriptors) built due to  $IC_{50}$  value for U251 cell line using multiple linear regressions (MLR) method is represented by the following equation:

$$PCI_{50} = 0.0011 + 0.1706 \text{ AM1\_dipole} + 0.0219 \text{ AM1\_humo} \quad \text{model (2)}$$

#### 3.1.2 Validation of the Models:

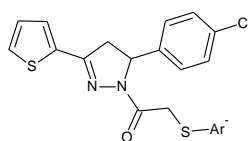
Table (3.1) validation models

	S	R <sup>2</sup>	R <sup>2</sup> (adj)	R <sup>2</sup> (predi)
Model (1)	0.269838	74.30%	61.44%	41.49%
Model (2)	0.193578	75.92%	74.13%	42.73%

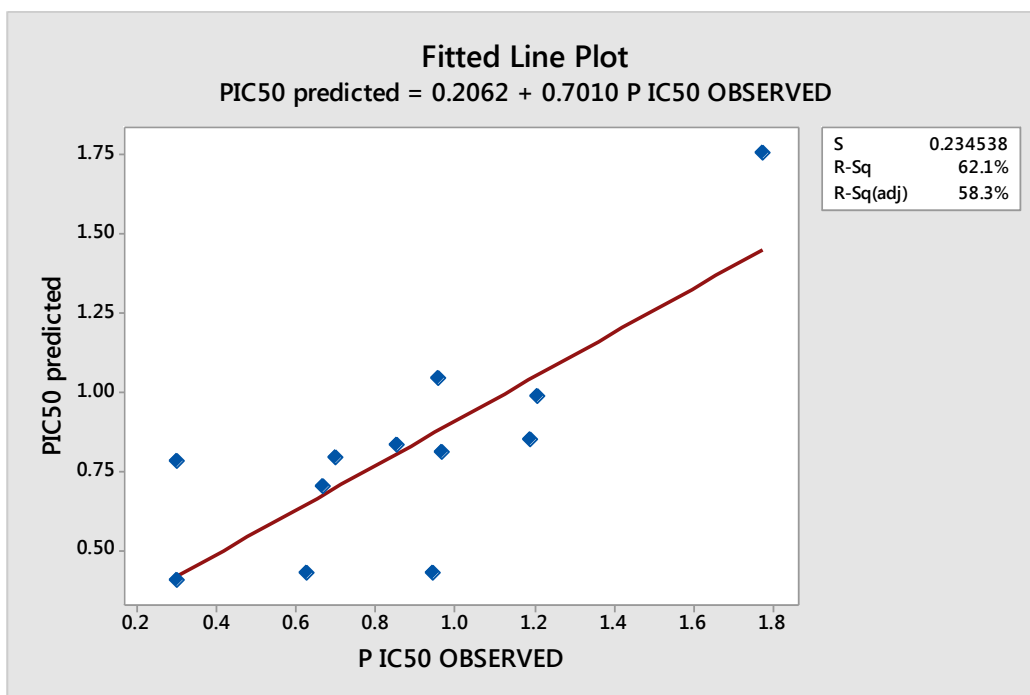
R-squared (R<sup>2</sup>) is a statistical measure of how close the data are to the fitted regression line.

For a statistically significant model, it is inevitable that the descriptors evolved in the equation should be least inter-correlated with each other, so the variance inflation factor (VIF) is the statistical factor detects multicollinearity in regression analysis. So the VIF values of these descriptors were found to be 1.81 for slog p and Slog\_VS4, 1.54 for formula weight and 1.23 for Model (1), and 3.32 for each of the AM1\_dipole and for AM1\_Humo in model (2) . All the VIF values were found to be less than 10, which suggest very less multicollinearity within descriptors.

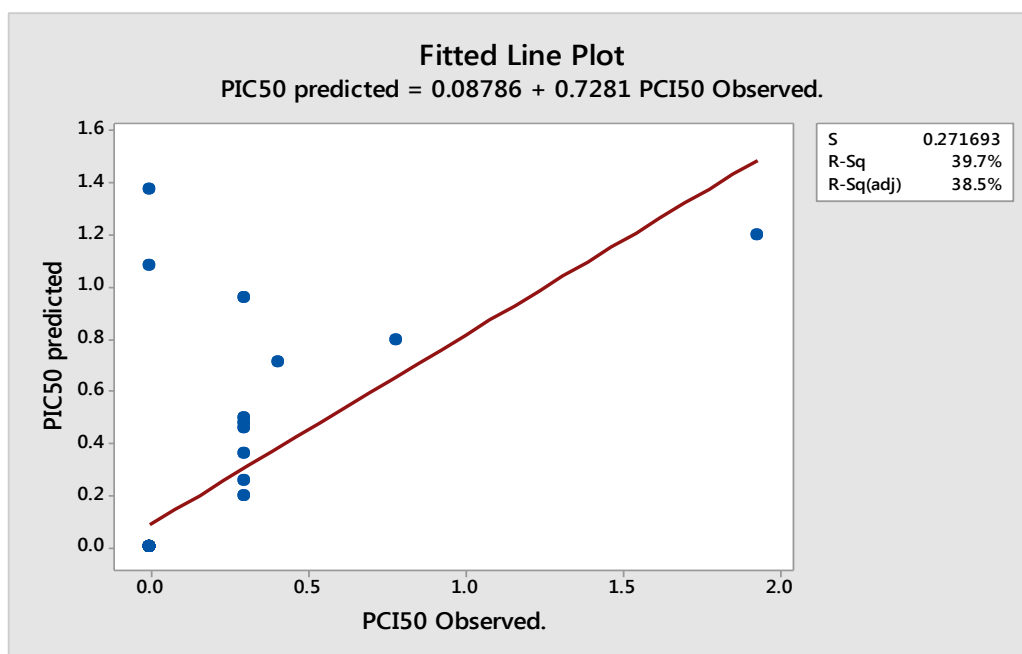
**Table (3.2) Predictive value (PIC<sub>50</sub>) of the data set through QSAR mod**



	Compound N.O	Ar	Predicted PIC <sub>50</sub> (mM)	
			AsPC-1 cell line	U251 cell line
Training set	1		0.407	0.181
	2		0.782	0.359
	3		0.853	0.532
	4		0.703	0.699
	5		0.794	0.871
	6		0.428	1.034
	7		0.832	1.214
	8		0.809	1.384
	9		1.042	1.559
	10		1.757	1.746
Test set	11		0.430	0.181
	12		0.990	1.082



**Figure (3.1) Predicted pancreatic anticancer activities by (MLR) in comparison with experimental values**



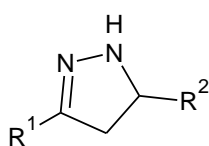
**Figure (3.2) Predicted glioblastoma anticancer activities by (MLR) in comparison with experimental values**



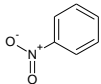
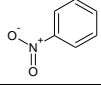

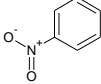
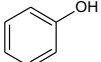
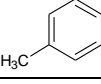
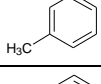
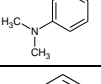
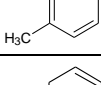
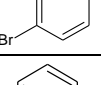
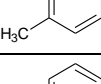
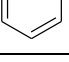
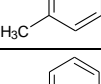
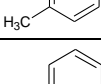
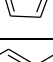
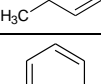
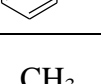
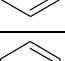
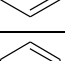
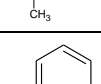
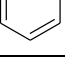
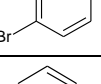
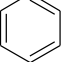
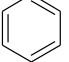
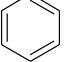
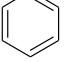

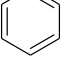
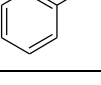
A good correlation was obtained with cross validation  $R^2=74.3$  and 75.92% for model 1 (AsPC-1 cell line) and model 2 (U251 human glioblastoma cell lines) respectively. So the predictive power of this model is significantly good.

The most important result of this investigation is that the anticancer activity could be predicted using QSAR methods. So, the model proposed in this study shows moderate predictive power, and the compounds which were designed show have abiological activity against AsPC-1 human pancreatic cell line and U251 human glioblastoma cell lines (table 3.3).

**Table (3.3) Predicated biological activity for the designed pyrazoline compounds**

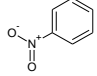
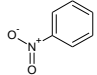
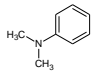
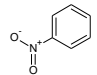
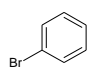
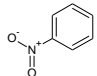
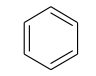
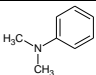
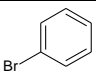
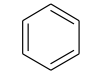
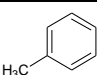
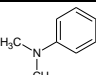


Compound N.O	R <sub>1</sub>	R <sub>2</sub>	AsPc_1 cell line		U251	
			PIC <sub>50</sub>	IC <sub>50</sub> (mM)	PIC50	IC <sub>50</sub> (mM)
VIII		CH <sub>3</sub>	-1.1698774	14.791	0.9549621	0.111
IX			0.28819248	0.515	1.2056068	0.062
X			0.5079702	0.31	0.7480286	0.179
XI			0.05948016	0.872	0.9238239	0.119
XII	CH <sub>3</sub>		-1.1213774	13.213	0.2870583	0.516
XIII	CH <sub>3</sub>		-0.9656777	9.247	0.2584296	0.552
XIV	CH <sub>3</sub>		-0.3853732	2.427	0.2182224	0.605
XV	CH <sub>3</sub>	CH <sub>3</sub>	-2.6114864	408.319	0.2600319	0.55
XVI	CH <sub>3</sub>	H	-2.7028536	504.661	0.2670587	0.541
XVII	CH <sub>3</sub>		-0.8584494	7.211	0.1654079	0.683
XVIII	CH <sub>3</sub>		-1.3118312	20.512	0.2865938	0.516

Compound N.O	R <sub>1</sub>	R <sub>2</sub>	AsPc_1 cell line		U251	
			PIC <sub>50</sub>	IC <sub>50</sub> (mM)	PIC <sub>50</sub>	IC <sub>50</sub> (mM)
XIX		H	-1.2612447	18.239	0.9199714	0.12
XX			0.58315956	0.261	0.8844531	0.131
XXI			0.12977776	0.742	0.868353	0.136
XXII		CH <sub>3</sub>	-0.476262	2.992	0.2218841	0.599
XXIII			0.98178159	0.104	0.2125886	0.612
XXIV			1.20156455	0.0623	0.2931519	0.509
XXV			0.75307451	0.177	0.2031738	0.627
XXVI		H	-0.5676293	3.698	0.23033	0.589
XXVII			1.27677496	0.053	0.1480144	0.711
XXVIII			0.82860687	0.148	0.2732726	0.533
XXIX		CH <sub>3</sub>	-1.4014389	25.176	0.2212892	0.601
XXX			0.056631	0.878	0.2426051	0.571
XXXI			0.26873828	0.538	0.4940453	0.321
XXXII			-0.1720813	1.486	0.1962743	0.637
XXXIII		H	-1.4928114	31.117	0.2304737	0.588
XXXIV			0.35159284	0.445	0.267586	0.54
XXXV			-0.101789	1.265	0.2593676	0.551

### 3.2 Docking output:

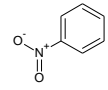
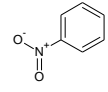
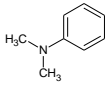
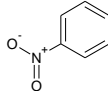
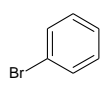
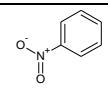
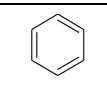
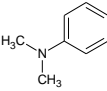
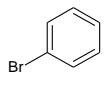
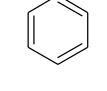
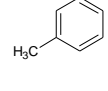
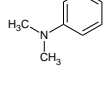
Table (3.4) Output of the Interaction between the ligand with 5kk5 protein active sides:

Compound N.O	R <sub>1</sub>	R <sub>2</sub>	Estimated free energy of binding (kcal/mol)	Interactions	
				H-bond	Induced dipole interaction
VIII		CH <sub>3</sub>	-10.67	—	—
IX			-18.57	—	Lys 570
X			-17.445	Ser A542	—
XI			-16.864	Ser A542	—
XII	CH <sub>3</sub>		-12.94	Lys A177	—
XIII	CH <sub>3</sub>		-14.402	—	—
XIV	CH <sub>3</sub>		-12.947	—	—
XXIII			-16.66	Ser A542	—

From the interaction of the ligand with 5kk5 protein active side results (table 3.4) showed that compounds X, XI and XIII were observed to have hydrogen bonding between nitrogen atom of the ligand with residue Ser A542 (figures 3.5 and 3.6 respectively). Residue LysA177 showed also hydrogen bond interaction with the nitrogen atom of the ligand with compound XIII (figure 3.8). Compound IX was observed to display induced dipole interaction with residue Lys 570.

The strength of a single hydrogen bond usually varies from 2 to 5kcal/mol. Hence formation of single hydrogen bond is relatively weak. However, a significant amount of bonding stability can be achieved when there is formation of multiple hydrogen bonds between two such systems (Roy, K.; *et al* 2015).

**Table (3.5) Output of the Interaction of the ligand with 1NQU protein active side:**

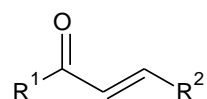
Compound N.O	R <sub>1</sub>	R <sub>2</sub>	Estimated free energy of binding (kcal/mol)	Interactions	
				pi-pi ( $\pi$ - $\pi$ ) stacking	Induced dipole interaction
VIII		CH <sub>3</sub>	-17.0292	Phe 22 (arene-arene)	—
IX			-20.81	Phe 22; Trp 57 (arene-arene)	Hiss 88
X			-19.3455	Phe 22; Trp 57 (arene-arene)	—
XI			-18.1315	Phe 22; Trp 57 (arene-arene)	—
XII	CH <sub>3</sub>		-15.5401	Phe 22 (arene-arene)	—
XIII	CH <sub>3</sub>		-15.8141	—	Hiss 88
XIV	CH <sub>3</sub>		-14.8892	Phe 22 (arene-arene)	—
XXIII			-18.39	Phe 22; Trp 57 (arene-arene)	Hiss 88

From the interaction of the ligand with 1NQU protein active side results (table 3.5), both compound (IX) and (XXIII) were observed displayed pi-pi stacking interaction with residue Phe 22 and Trp 57 (figures 3.32 and 3.56). This refers to a special type of non-covalent attractive force due to overlapping of the orbital occurring between compounds possessing un-saturation; that is pi electrons. This interaction provides stability to proteins containing aromatic amino acid (Roy, K.; *etal* 2015). On another hand compounds (IX) and (XXIII) observed to have induce dipole interaction between nitrogen atoms of the lignd with residue Hiss 88. Comparing between compound IX and XXIII showed the same interaction clearly can observed the existence of withdrawing group (nitro) in compound IX shows high binding score (-20.81 kcal/mol) while the existence of donating group (methyl) shows less binding score (-18.39 kcal/mol).

Compounds X and IX were found to be the most effective anticancer agent against AsPC-1 and U251 cell lines, with IC<sub>50</sub> values 0.31mM and 0.062mM respectively.

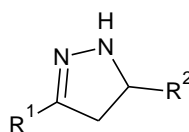
### 3.3 Synthesis of Pyrazoline Compounds:

**Table (3.6) Reaction conditions of synthesized enone compounds:**



Compound N.O	R1	R2	Reaction time	Yield (g)	Yield (%)	Color	M.wt	M.P(C°)
I		CH <sub>3</sub>	10 min	0.28	58.58	brown	191.2	64-69
II			1 hour	0.67	90.4	Dark red	296.34	190-194
III			1 hour	0.78	93.8	Yellow	332.17	155-158
IV			5 min	0.53	79.9	brown	253.27	118-123
V	CH <sub>3</sub>		2 mint	0.37	84.09	Orange	189.27	75-77
VI	CH <sub>3</sub>		10 min	0.46	84.1	Light yellow	255.1	190-195
VII	CH <sub>3</sub>		15 min	0.15	41.0	Beige	146.2	97-100

- All the structures of the compounds were elucidated by IR, TLC, UV and melting point.

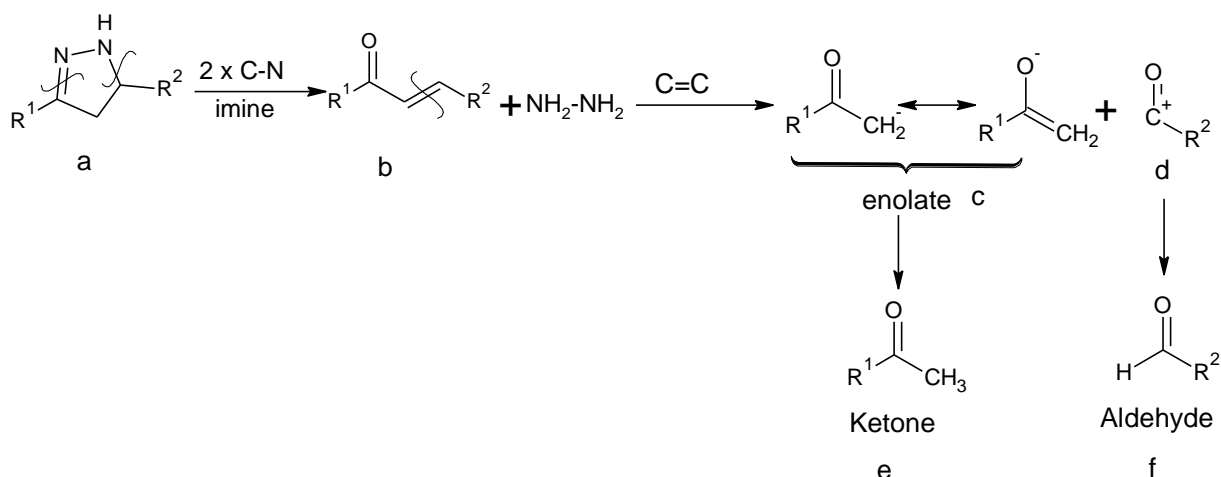
**Table (3.7) Reaction conditions of pyrazolines compounds**

Compound N.O	R1	R2	Reaction time	Yield (g)	Yield (%)	Color	M.wt	M.P(C°)
VIII		CH <sub>3</sub>	20 min	0.13	100.78	brown	205.21	145-150
IX			30 min	0.38	98.7	Dark red	310.35	159-161
X			30 min	0.74	88.76	Orange	346.18	137-145
XI			10 min	0.05	93.6	Dark yellow	267.28	83-85
XII	CH <sub>3</sub>		15 min	0.16	124.03	brown	203.28	189-192
XIII	CH <sub>3</sub>		30 min	0.11	73.83	Light yellow	239.11	84-93
XIV	CH <sub>3</sub>		30 min	0.04	73.43	Yellow	160.22	125-130

- All the structures of the compounds were elucidated by IR, TLC, UV and melting point.

A series of some enone and 3, 5 di-substituted pyrazoline derivatives were successfully synthesized by using grinding as one of the solvent free methodologies. The results was obtained show that this method has given a high yields (Tables 3.6 and 3.7), all the compounds was successfully syntheized which were elucidated by TLC, IR and U.V.

### 3.3.1 Retro synthetic analysis (RSA) of Pyrazoline:

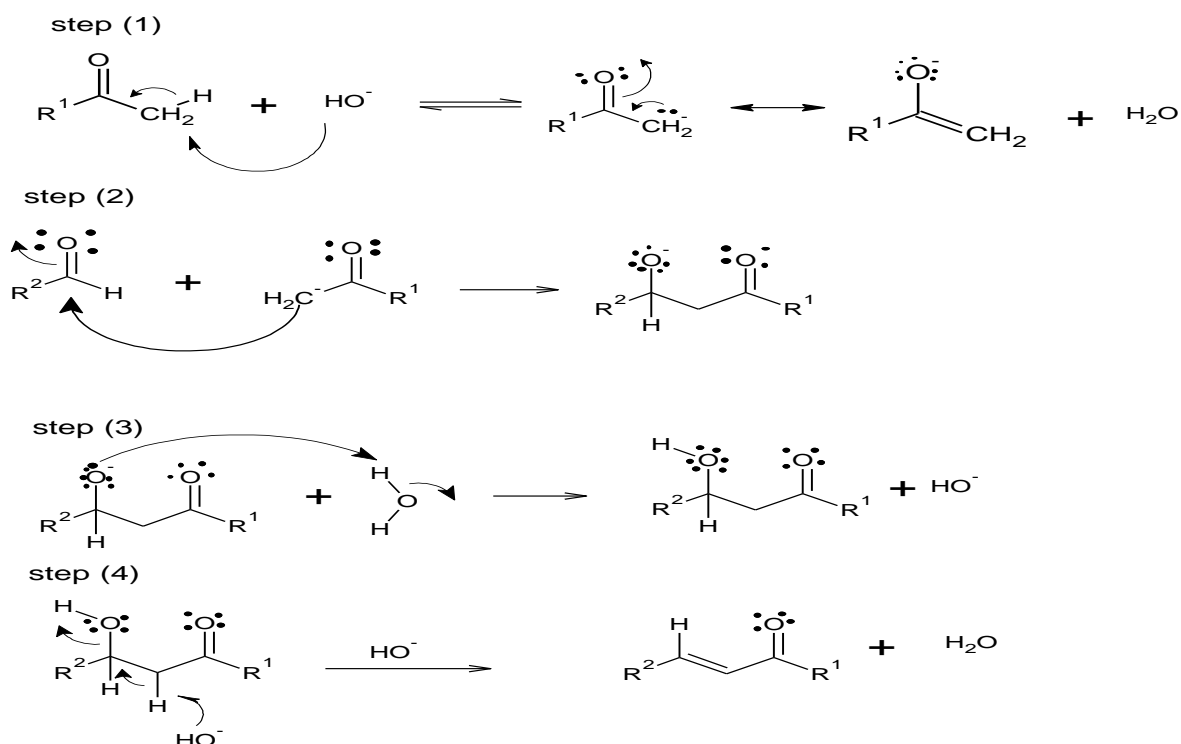


**Scheme (3.1) Pyrazoline retro synthetic analysis**

By the disconnection of two C-N bonds of imine (a) we get back of enone (b), the disconnection of C=C of the enone (b) gives the nucleophile enolate (c) and electrophile (d) which are the synthones of the reagents ketone (e) and aldehyde (f) respectively (Warren, S. Wyatt, P., 2008).

### 3.3.2 Mechanism:

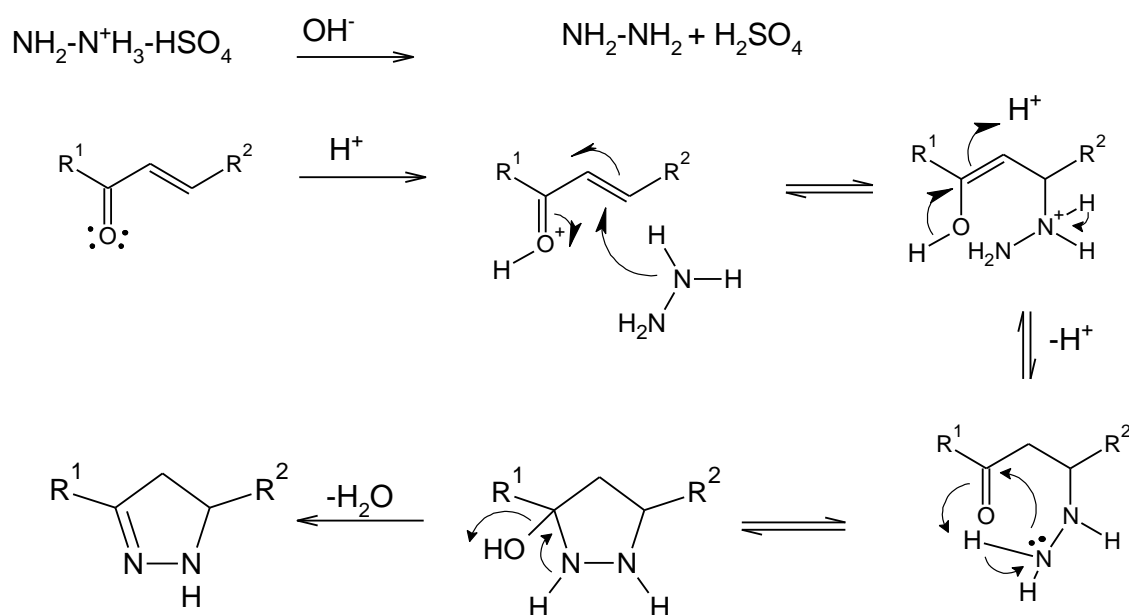
#### 3.3.2.1 Mechanism of Enone Synthesis:



**Scheme (3.2) Claisen-Schmidt condensation mechanism**

The first step involves the acid-base reaction between a strong base (hydroxide ion) and a hydrogen located alpha to a ketone carbonyl group to generate an enolate form. The step (2) the enolate attacks the carbonyl group of the aldehyde (nucleophilic addition). Then the reaction undergoes an acid-base reaction with the remaining acidic alpha-hydrogen, followed by the loss of  $\text{OH}^-$  as a leaving group to give an enone, which has the alkene and the ketone functional groups (step 3 and 4). The net loss of  $\text{H}^+$  and  $\text{OH}^-$  represents the loss of water.

### 3.3.2.2 Mechanism of Pyrazoline Synthesis:



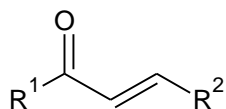
**Scheme (3.3) Pyrazoline synthesis mechanism**

The first step involves the protonation of the carbonyl group ( $\text{H}^+$  is a hard cation, prefers 1,2 addition over 1,4 addition), according to the nature of the electrophile (enone) and particularly steric hindrance around the carbonyl group, the 1,4 conjugate addition is favorable, followed by loss of  $\text{H}^+$ . The ring closure reaction is obtained by the 1,2 direct addition, followed by loss of a water molecule (Patai, S., Rappoport, Z. 1989).



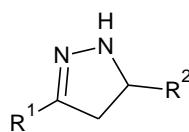
### 3.3.3 Characterizations of the Compounds:

**Table (3.8) Physical parameters of synthesized enone compounds**



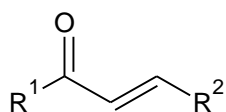
Compound N.O	R1	R2	R.F Value	Solvent system (n-hexane: ethyl acetate)	U.V (Ethanol 95%) λ max (nm)	Melting point C°
I		CH <sub>3</sub>	0.95	1:3	288	64-69
II			0.45	3:1	458	190-194
III			0.78	3:1	333	155-158
IV			0.90	1:3	310	118-123
V	CH <sub>3</sub>		0.88	1:3	349	75-77
VI	CH <sub>3</sub>		0.72	3:1	336	190-195
VII	CH <sub>3</sub>		0.70	3:1	326	97-100

Table (3.9) shows Physical parameters of synthesized Pyrazolines:



Compound N.O	R <sub>1</sub>	R <sub>2</sub>	R.F Value	Solvent system (n-hexane: ethyl acetate)	U.V (Ethanol 75%) λ <sub>max</sub> (nm)	Melting point C°
VIII		CH <sub>3</sub>	0.93	1:3	309	145-150
IX			0.22	3:1	294	159-161
X			0.55	3:1	324	137-145
XI			0.85	1:3	331	83-85
XII	CH <sub>3</sub>		0.90	1:3	398	189-192
XIII	CH <sub>3</sub>		0.70	1:3	337	84-93
XIV	CH <sub>3</sub>		0.61	1:3	302	125-130

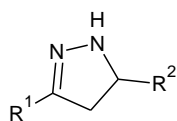
**Table (3.10) shows the IR spectrum data of enone compounds**



IR (KBr)  $\nu$  max (cm<sup>-1</sup>)

Compound N.O	R <sub>1</sub>	R <sub>2</sub>	C=O St.vib	C=C St.vib	C-H St.vib	C-H bending	O-N=O asym	O-N=O sym
I		CH <sub>3</sub>	1690	1600	3104 (SP <sup>2</sup> )	1399	1522	1347
II			1648	1564	2906	1440	1523	1336
III			1662	1593	—	—	1517	1327
IV			1663	1599	—	—	1516	1335
V	CH <sub>3</sub>		1666	1599	2909	1438	—	—
VI	CH <sub>3</sub>		1649	1549	2918	1486	—	—
VII	CH <sub>3</sub>		1706	1660	3028 (SP <sup>2</sup> ), 2916	1449	—	—

**Table (3.11) shows the IR spectrum data of synthesized Pyrazolines**



IR (KBr)  $\nu$  max (cm<sup>-1</sup>)

Compound N.O	R <sub>1</sub>	R <sub>2</sub>	C=N St.vib	N-H St.vib	C-H St.vib	C-H Bending	O-N=O asym	O-N=O sym	C-N St.vib
VIII		CH <sub>3</sub>	1588	3396	—	1403	1515	1342	—
IX			1566	3425	2917	1434	1524	1314	1179
X			1657	3425	—	—	1518	1335	—
XI			1599	3423	—	—	1517	1340	1140
XII	CH <sub>3</sub>		1500	3430	2916	—	—	—	—
XIII	CH <sub>3</sub>		1591	—	2915	1484	—	—	1185
XIV	CH <sub>3</sub>		1602	3437	—	1406	—	—	1134

### 3.3.3.1 Thin Layer Chromatography:

According to the experiment, the solvent system is employed in order to dissolve and assist the compounds to move along the silica plate by capillary action. In solvent system mixture of 70% of n-hexane and 30% of ethyl acetate showed less polarity compared with solvent system mixture of 30% n-hexane and 70% ethyl acetate, due to the presence of 70 part of non-polar n-hexane in 30 part of polar ethyl acetate which slightly decreases the polarity of the overall solvent. This is also decrease the movement of the sample by capillary action through the stationary phase (moisture adsorbed by silica gel).

From the results, tables (3.8) and (3.9) the differences on the R<sub>f</sub> value verify the formation of Pyrazoline compound.

### 3.3.3.2 Ultra Violet/Visible Spectroscopy:

Light in the ultraviolet-visible (UV-Vis) region of the electromagnetic spectrum (200 – 800 nm) can affect the electronic transitions.

Absorbed UV-Vis energy is strong enough to actually excite an electron from a low-lying bonding/nonbonding orbital to a higher-lying antibonding orbital. The energy of the transition (or the difference in energy between the ground state and excited state energy levels) is measured by the wavelength of the absorbed light ( $\lambda_{\text{max}}$ ).

From the results obtained both enone and pyrazolines compounds show the absorption in the visible region from (288 – 458 nm) and (298-398nm) tables (3.8) and (3.9) respectively, as transition from  $\pi$ - $\pi^*$ . Due to the conjugated systems the  $\pi$  electrons of the double bond are delocalized, the HOMO-LUMO gap decreases as conjugation increases, shifting  $\lambda_{\text{max}}$  to longer wavelengths.

For molecules having conjugated systems of electrons, the ground states and excited states of the electrons are closer in energy than for non-conjugated systems. This means that lower energy light is needed to excite electrons in conjugated systems, which means that lower energy light is absorbed by conjugated systems. So a highly conjugated system then might absorb the lower energy portions of the light and reflect what is not absorbed. It is this reflected portion that the eye will perceive as the color of that object. A less highly conjugated system will require the absorption of the higher energy part of the spectrum, allowing the lower energy parts to be reflected to the eye. So this could explain the colors of the synthesized compounds; this is clearly observed in compound (II).

### 3.3.3.3 Infra-Red:

Table (3.10) IR spectrum of enone shows the absorption of the carbonyl group st.vib between ( $1648\text{-}1706\text{cm}^{-1}$ ) and the alkene group (C=C) st.vib absorption in the range ( $1600\text{-}1546\text{cm}^{-1}$ ) it proved of successfully synthesized enone. It clearly observed that the absorption of carbonyl group (C=O) st.vib was present in range that is less than the characteristic absorption of aldehyde ( $1725\text{ cm}^{-1}$ ), this due to the presence of the conjugated system. Table (3.11) IR spectrum of Pyrazoline showed mainly the absence of the carbonyl st.vib absorption with the presence of imines (C=N)  $1500\text{-}1657\text{cm}^{-1}$  absorption. This proved that the Pyrazolines is successfully synthesized.

**Conclusion:**

Some of Pyrazoline derivatives were modeled and investigated for their anticancer activity on AsPC-1 human pancreatic, and U251 human glioblastoma cell lines through QSAR and molecular docking or protein ligand interaction. Compounds X and IX showed the best result against AsPC-1 and U251 cell lines, with IC<sub>50</sub> values 0.31mM and 0.062mM respectively.

**Recommendations:**

In the view of this study we recommended H<sup>1</sup>-NMR, C<sup>13</sup>-NMR and mass spectroscopy as further characterization assay to the synthesized compounds. Moreover research can be carried out on the development of strong effective anticancer agents by modify to the structures of these compounds.

# References

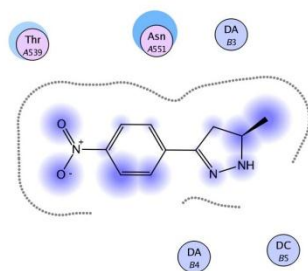
## References:

- Bora,U; Saikia, A; and Boruah, R.C; (2005), A new protocol for synthesis of  $\alpha$ ,  $\beta$ -unsaturated ketones using zirconium tetrachloride under microwave irradiation, *J. Indian Journal of chemistry*, (44B), 2523.
  
- Jasril, J; Ikhtiarudin, I; Zamri, A; Teruna, H.Y. and Frimayanti, N. (2017), New fluorinated chalcone and pyrazoline analogs: Synthesis, docking, and molecular dynamic studies as anticancer agents, *Journal of Pharmaceutical Sciences*, (41), 96.
  
- Jayaropa, P. (2013), Synthesis, characterization and biological studies of five membered nitrogen heterocycles, *Journal of Shodhgana*, (4), 131.
  
- Junghare, N. A. (2001), Synthesis and Reactivity of 3 Aroyl flavanones and 3 Aroyl Flavones, *Journal of Shodhgana*, (2), 64-66.
  
- Karabacak, M; Altintop, M.D; Ciftci, H.I; Koga, R; Otsuka, M; Fujita, M. and Ozdemir, A. (2015), Synthesis and Evaluation of New Pyrazoline Derivatives as Potential Anticancer Agents, *Journal of molecules*, (20), 19068-19071.
  
- Lewars, E.G. (2004), *Computational Chemistry Introduction to the Theory and Applications of Molecular and Quantum Mechanics*, (116), xvii-3.
  
- Nagendrappa,P. (2002), Organic synthesis under solvent-free condition. An environmentally benign procedure-1, *Journal of Resonance*, (7) (10), 59-61.
  
- Patai, S., Rappoport, Z., (1989), *The Chemistry of Enone*, 356-357.
  
- Roy, K.; Kar, S.; and Das, R.N. (2015), Understanding the basic of QSAR for applications in Pharmaceutical sciences and risk assessment, 31, 52-60.
  
- Samira, M; Dguigui, K. and Menana, E. (2011), Construction of 3D-QSAR models to predict antiamebic activities of pyrazoline and dioxazoles derivatives, *Journal of Materials and Environmental Science*, (2)(1), 62.
  
- Soni, H.M; Patel, P.K; Chhabria, M.T; Rana, D.N; Mahajan, B.M. and Brahmshatriya, P.S. (2015), 2D-QSAR Study of a Series of Pyrazoline-Based Anti-Tubercular Agents Using Genetic Function Approximation, *Journal of Computational chemistry*, (3), 46.

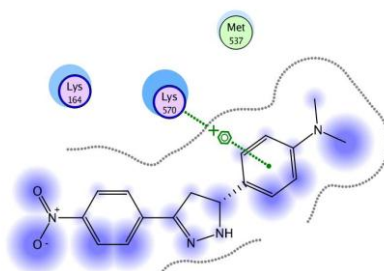


- Warren, S., Wyatt, P., (2008), Organic Synthesis: The disconnection Approach, 301-302.
- Young, D.C. (2001), CHEMISTRY COMPUTATIONAL CHEMISTRY A Practical Guide for Applying Techniques to Real-World Problems, (9), 1.

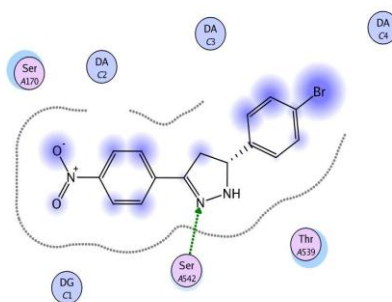
# **Appendixes**



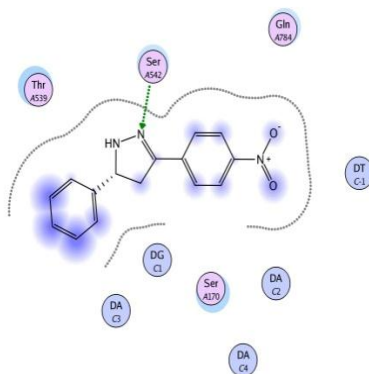
**Figure (3.3) show the interactions between the ligand (compound VIII) and the 5kk5 protein active side**



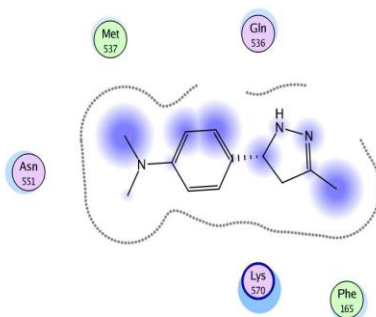
**Figure (3.4) show the interactions between the ligand (compound IX) and the 5kk5 protein active side**



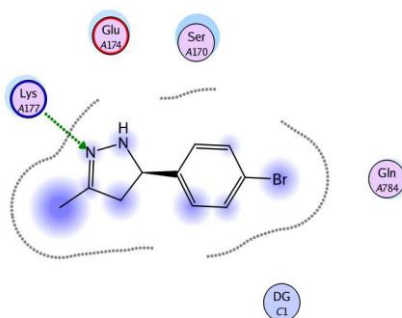
**Figure (3.5) show the interactions between the ligand (compound X) and the 5kk5 protein active side**



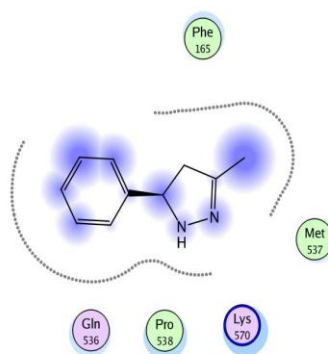
**Figure (3.6) show the interactions between the ligand (compound XI) and the 5kk5 protein active side**



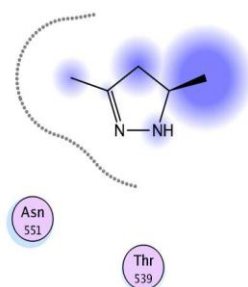
**Figure (3.7) show the interactions between the ligand (compound XII) and the 5kk5 protein active side**



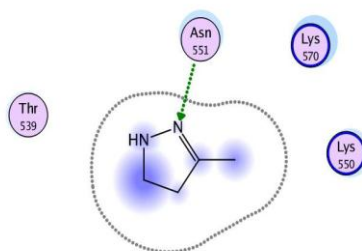
**Figure (3.8) show the interactions between the ligand (compound XIII) and the 5kk5 protein active side**



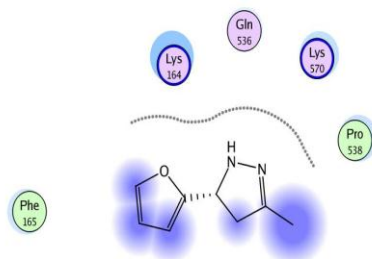
**Figure (3.9) show the interactions between the ligand (compound XIV) and the 5kk5 protein active side**



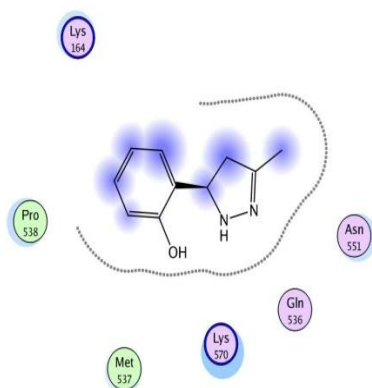
**Figure (3.10) show the interactions between the ligand (compound XV) and the 5kk5 protein active side**



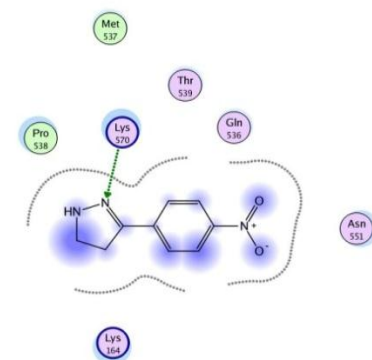
**Figure (3.11) show the interactions between the ligand (compound XVI) and the 5kk5 protein active side**



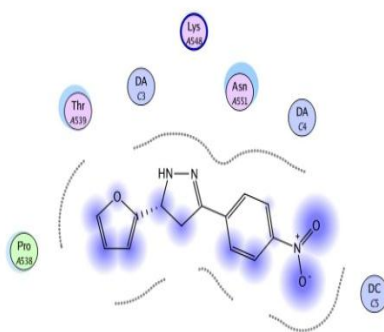
**Figure (3.12) show the interactions between the ligand (compound XVII) and the 5kk5 protein active side**



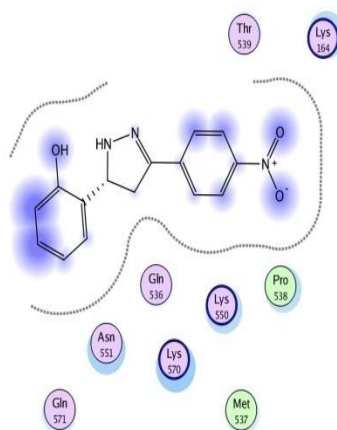
**Figure (3.13) show the interactions between the ligand (compound XVIII) and the 5kk5 protein active side**



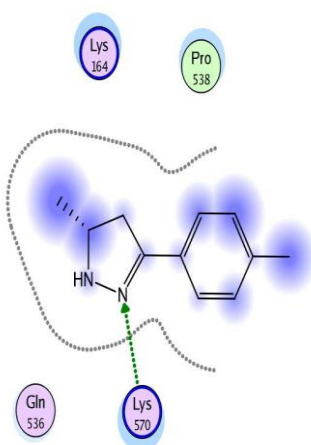
**Figure (3.14) show the interactions between the ligand (compound XIX) and the 5kk5 protein active side**



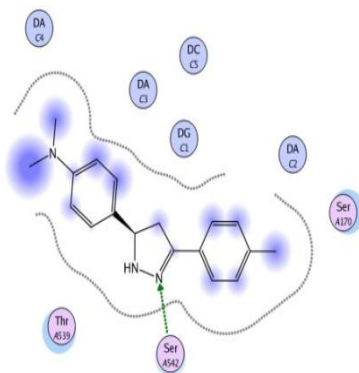
**Figure (3.15) show the interactions between the ligand (compound XX) and the 5k5 protein active side**



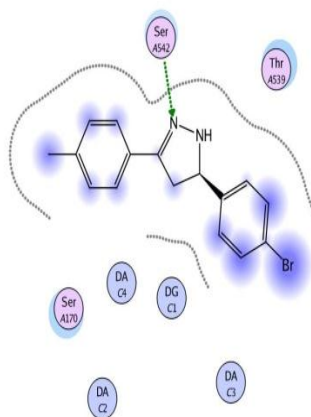
**Figure (3.16) show the interactions between the ligand (compound XXI) and the 5k5 protein active side**



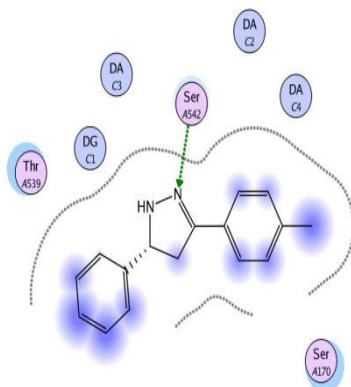
**Figure (3.17) show the interactions between the ligand (compound XXII) and the 5k5 protein active side**



**Figure (3.18) show the interactions between the ligand (compound XXIII) and the 5kk5 protein active side**

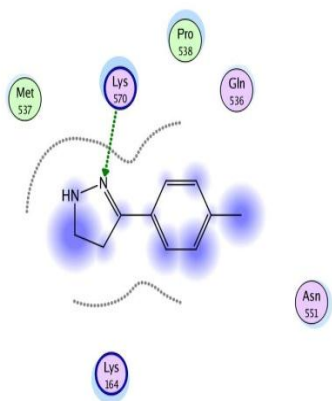


**Figure (3.19) show the interactions between the ligand (compound XXIV) and the 5kk5 protein active side**

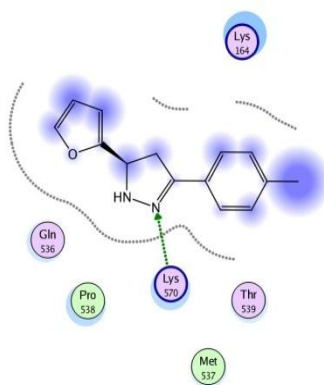


**Figure (3.20) show the interactions between the ligand (compound XXV) and the 5kk5 protein active side**

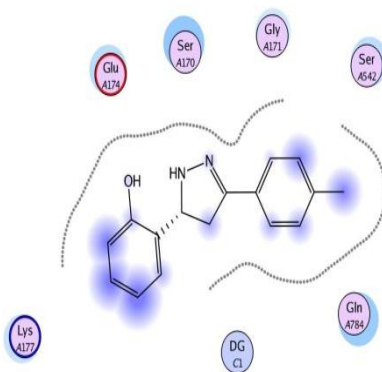




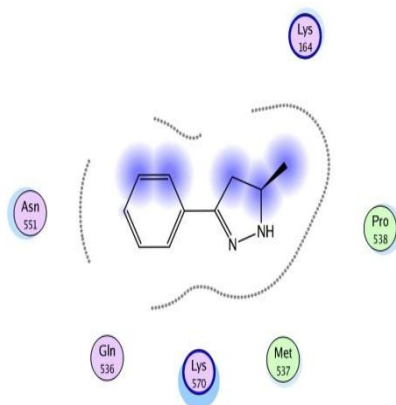
**Figure (3.21) show the interactions between the ligand (compound XXVI) and the 5kk5 protein active side**



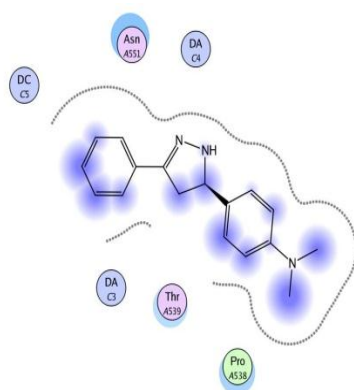
**Figure (3.22) show the interactions between the ligand (compound XXVII) and the 5kk5 protein active side**



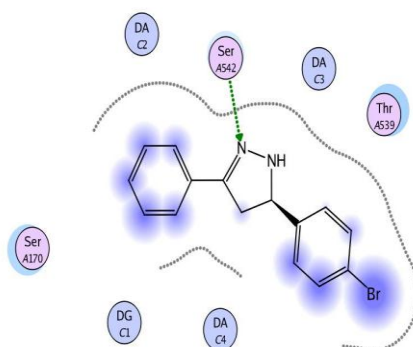
**Figure (3.23) show the interactions between the ligand (compound XXVIII) and the 5kk5 protein active side**



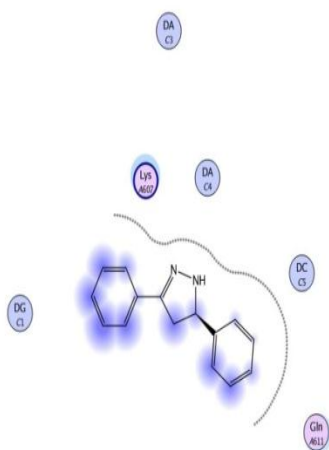
**Figure (3.24) show the interactions between the ligand (compound XXIX) and the 5kk5 protein active side**



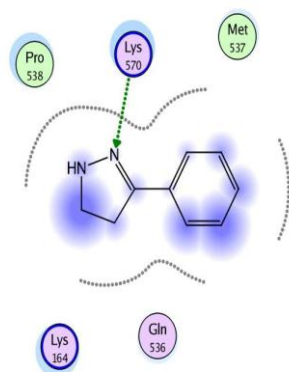
**Figure (3.25) show the interactions between the ligand (compound XXX) and the 5kk5 protein active side**



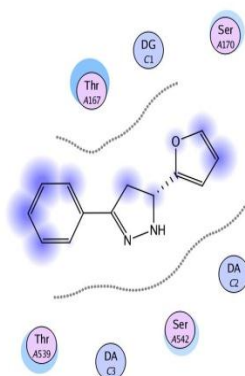
**Figure (3.26) show the interactions between the ligand (compound XXXI) and the 5kk5 protein active side**



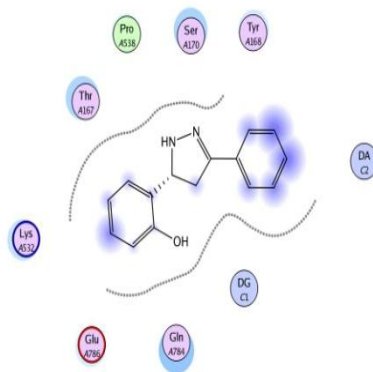
**Figure (3.27) show the interactions between the ligand (compound XXXII) and the 5kk5 protein active side**



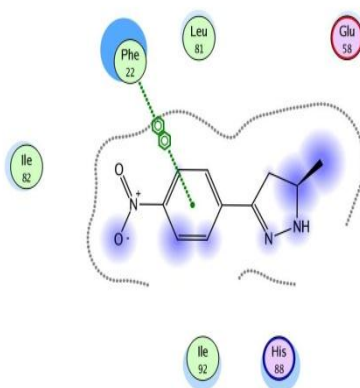
**Figure (3.28) show the interactions between the ligand (compound XXXIII) and the 5kk5 protein active side**



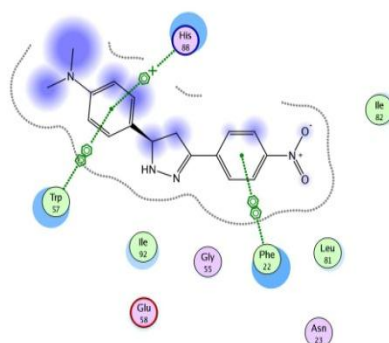
**Figure (3.29) show the interactions between the ligand (compound XXXIV) and the 5kk5 protein active side**



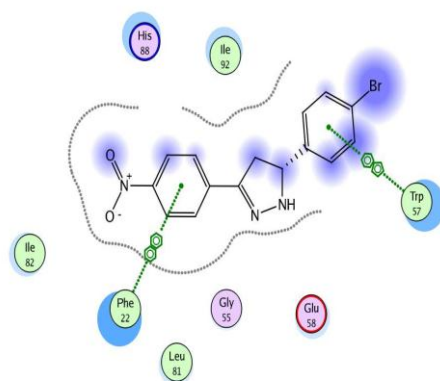
**Figure (3.30) show the interactions between the ligand (compound XXXV) and the 5kk5 protein active side**



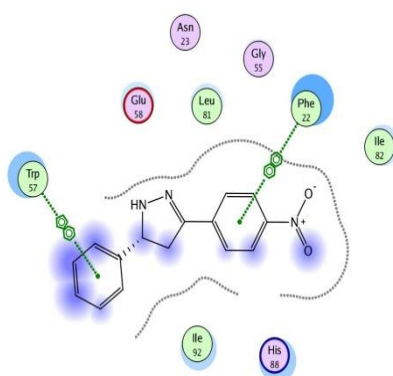
**Figure (3.31) show the interactions between the ligand (compound VIII) and the 1NQU protein active side**



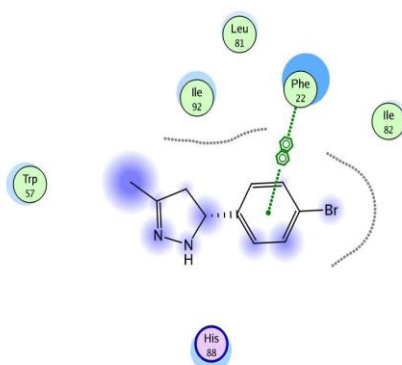
**Figure (3.32) show the interactions between the ligand (compound IX) and the 1NQU protein active side**



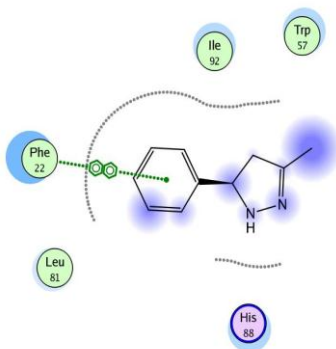
**Figure (3.33) show the interactions between the ligand (compound X) and the 1NQU protein active side**



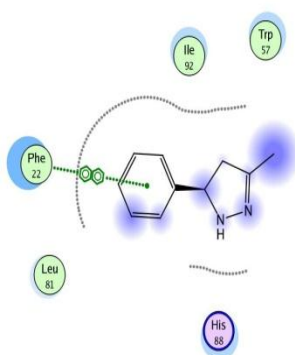
**Figure (3.34) show the interactions between the ligand (compound XI) and the 1NQU protein active side**



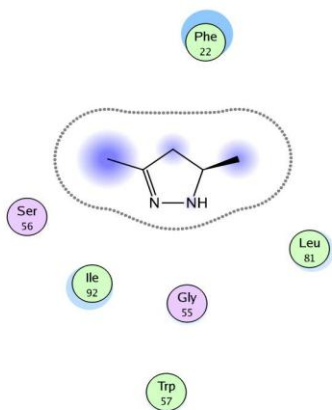
**Figure (3.35) show the interactions between the ligand (compound XII) and the 1NQU protein active side**



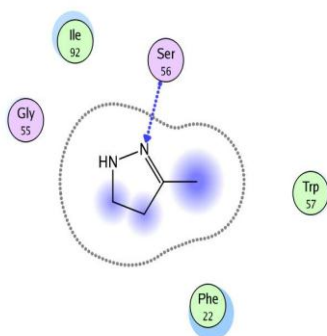
**Figure (3.36) show the interactions between the ligand (compound XIII) and the 1NQU protein active side**



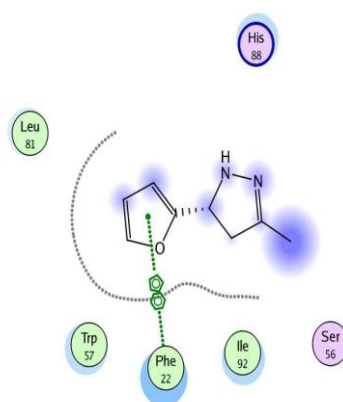
**Figure (3.37) show the interactions between the ligand (compound XIV) and the 1NQU protein active side**



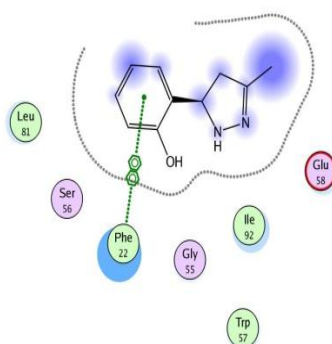
**Figure (3.38) show the interactions between the ligand (compound XV) and the 1NQU protein active side**



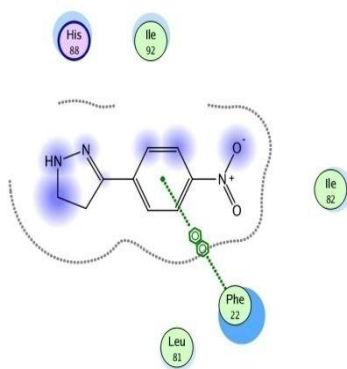
**Figure (3.39) show the interactions between the ligand (compound XVI) and the 1NQU protein active side**



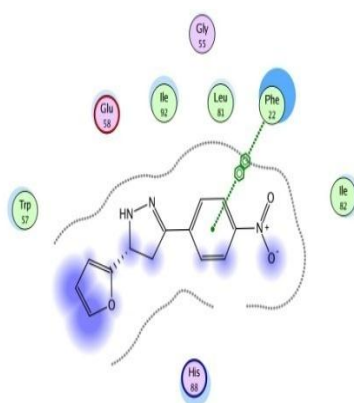
**Figure (3.40) show the interactions between the ligand (compound XVII) and the 1NQU protein active side**



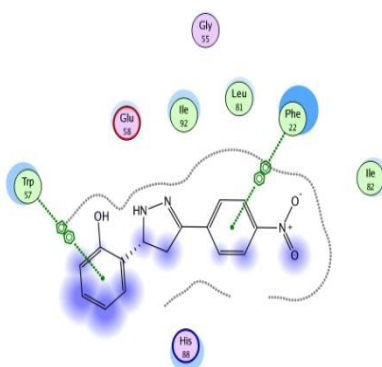
**Figure (3.41) show the interactions between the ligand (compound XVIII) and the 1NQU protein active side**



**Figure (3.42) show the interactions between the ligand (compound XIX) and the 1NQU protein active side**

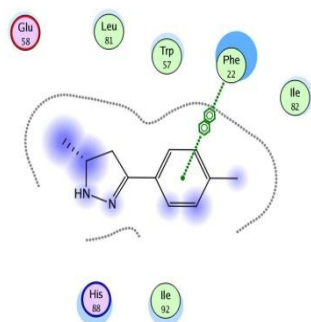


**Figure (3.43) show the interactions between the ligand (compound XX) and the 1NQU protein active side**

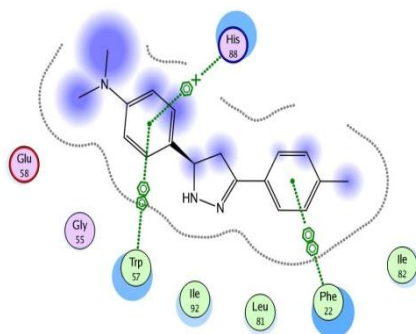


**Figure (3.44) show the interactions between the ligand (compound XXI) and the 1NQU protein active side**

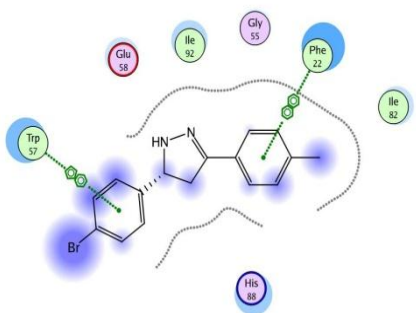




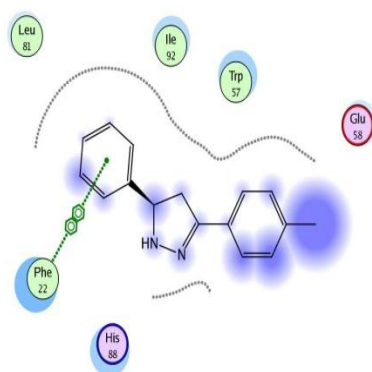
**Figure (3.45) show the interactions between the ligand (compound XXII) and the 1NQU protein active side**



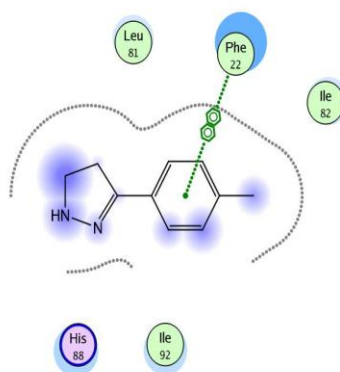
**Figure (3.46) show the interactions between the ligand (compound XXIII) and the 1NQU protein active side**



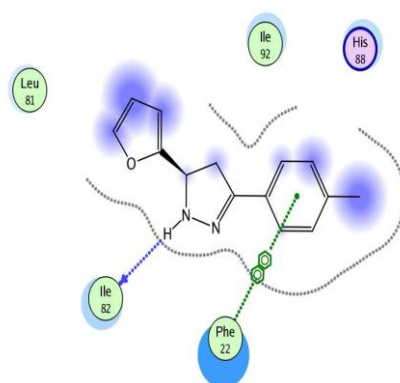
**Figure (3.47) show the interactions between the ligand (compound XXIV) and the 1NQU protein active side**



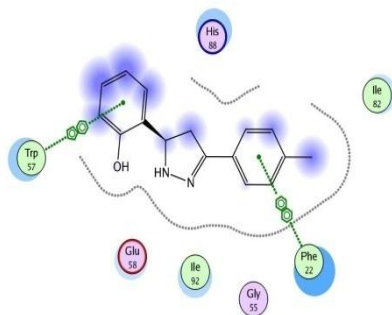
**Figure (3.48) show the interactions between the ligand (compound XXV) and the 1NQU protein active side**



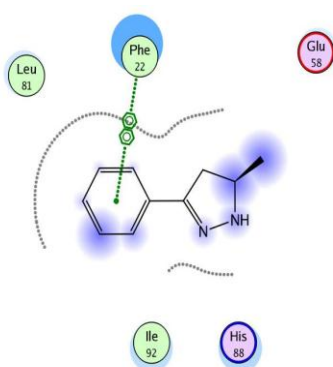
**Figure (3.49) show the interactions between the ligand (compound XXVI) and the 1NQU protein active side**



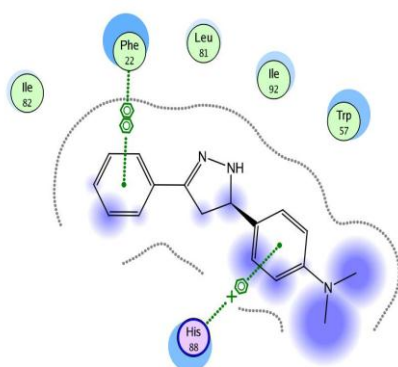
**Figure (3.50) show the interactions between the ligand (compound XXVII) and the 1NQU protein active side**



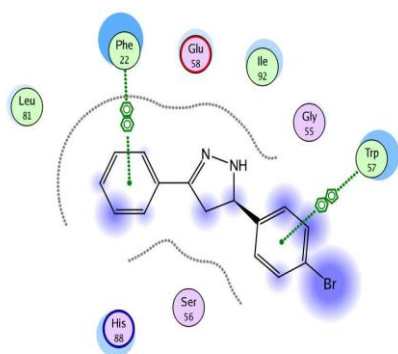
**Figure (3.51) show the interactions between the ligand (compound XXVIII) and the 1NQU protein active side**



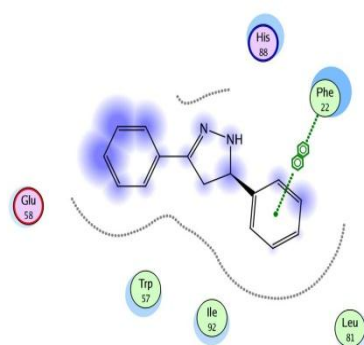
**Figure (3.52) show the interactions between the ligand (compound XXIX) and the 1NQU protein active side**



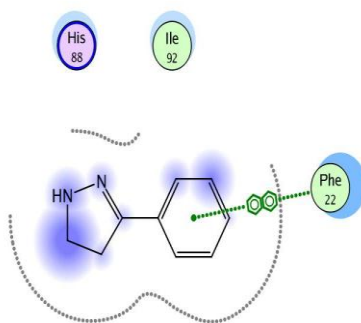
**Figure (3.53) show the interactions between the ligand (compound XXX) and the 1NQU protein active side**



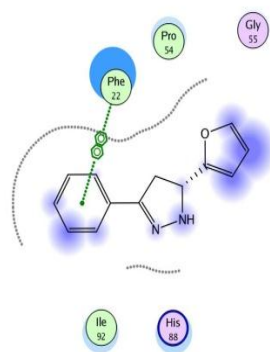
**Figure (3.54) show the interactions between the ligand (compound XXXI) and the 1NQU protein active side**



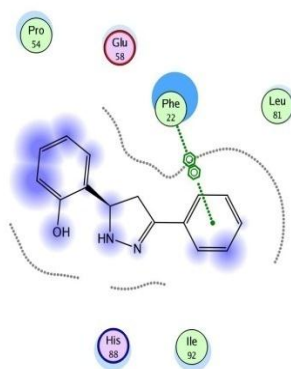
**Figure (3.55) show the interactions between the ligand (compound XXXII) and the 1NQU protein active side**



**Figure (3.56) show the interactions between the ligand (compound XXXIII) and the 1NQU protein active side**



**Figure (3.57) show the interactions between the ligand (compound XXXIV) and the 1NQU protein active side**



**Figure (3.58) show the interactions between the ligand (compound XXXV) and the 1NQU protein active side**

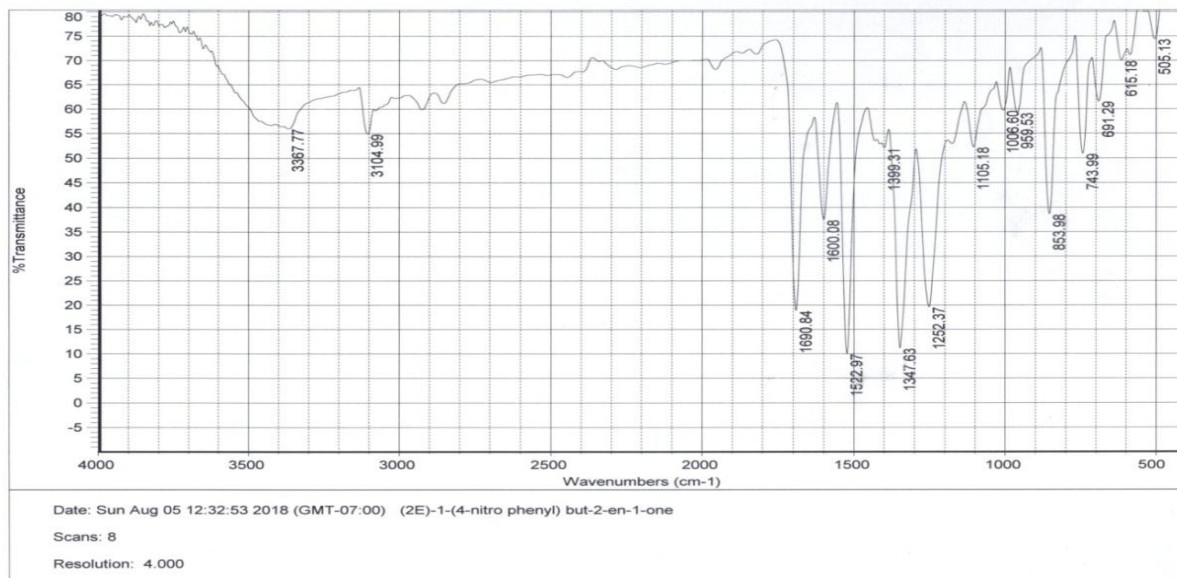


Figure (3.59) show the IR spectrum of compound I

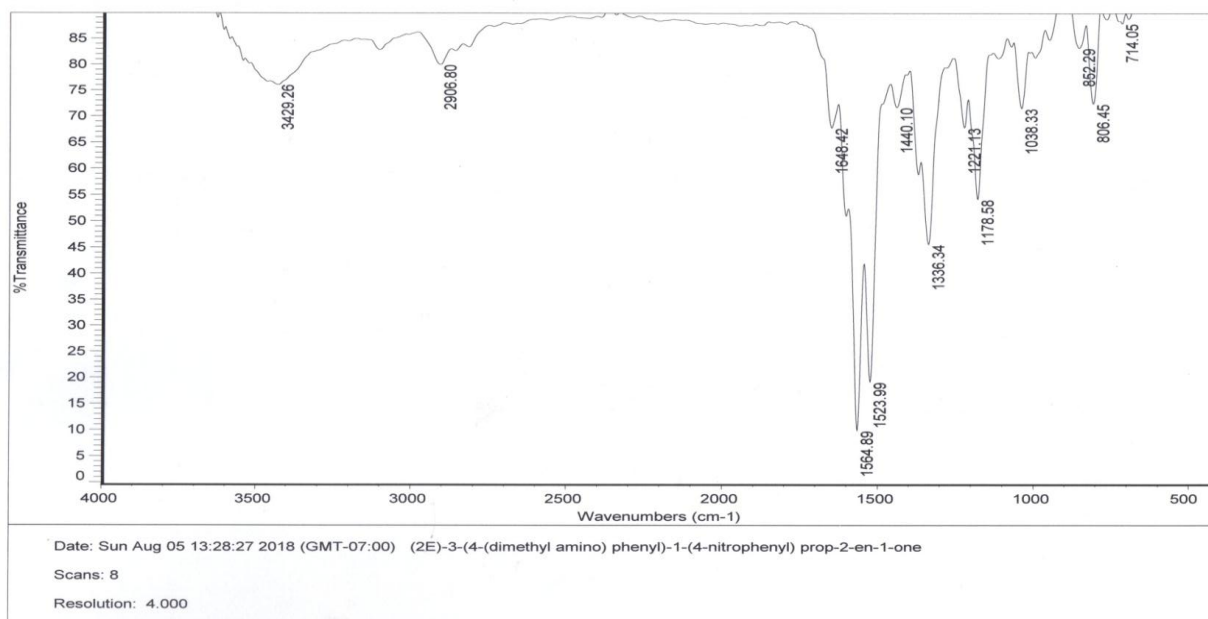


Figure (3.60) show the IR spectrum of compound II

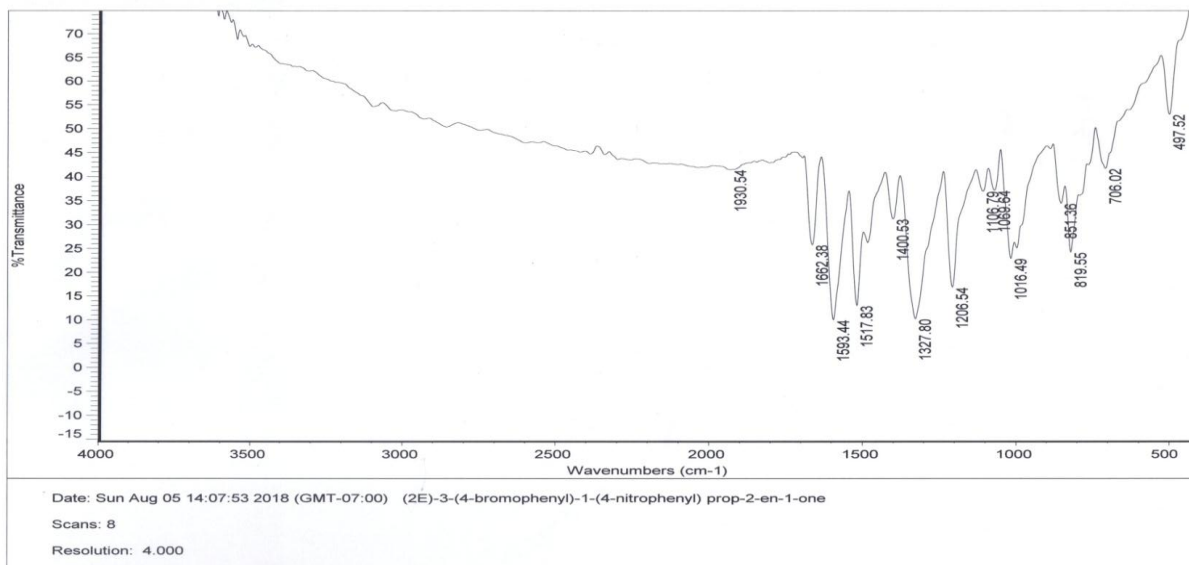


Figure (3.61) show the IR spectrum of compound III

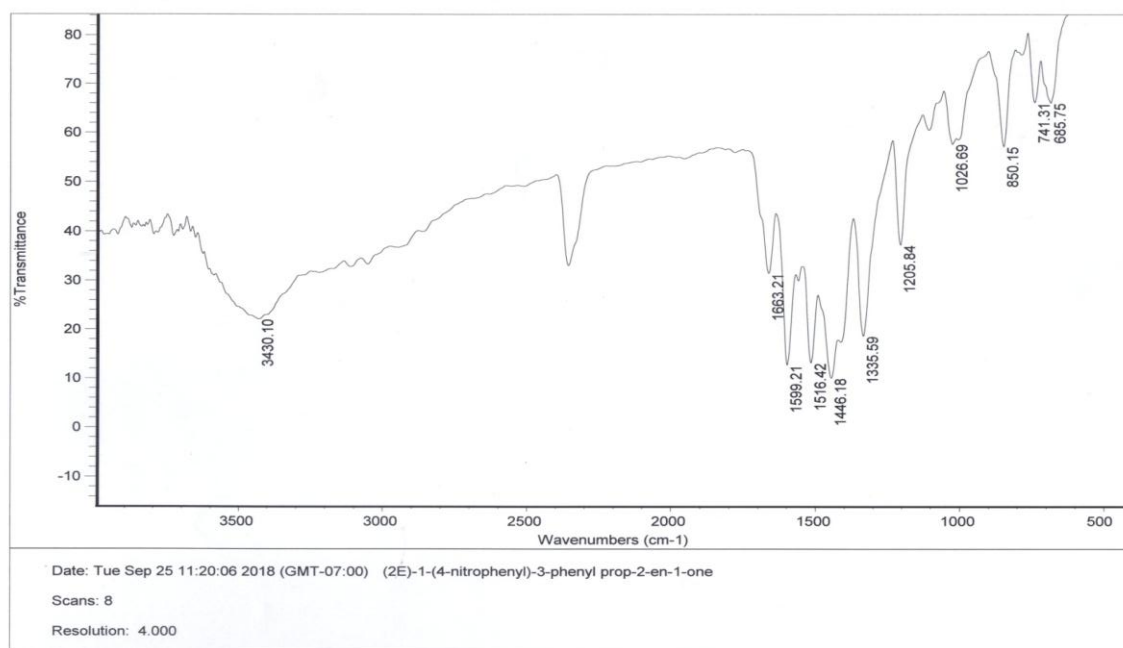


Figure (3.62) show the IR spectrum of compound IV

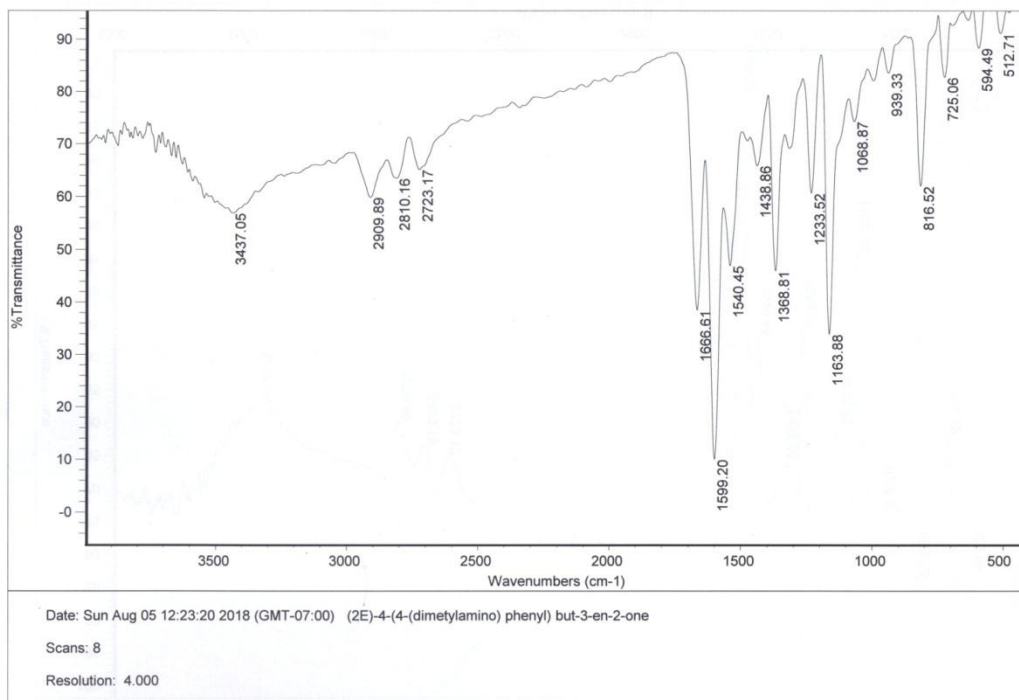


Figure (3.63) show the IR spectrum of compound V

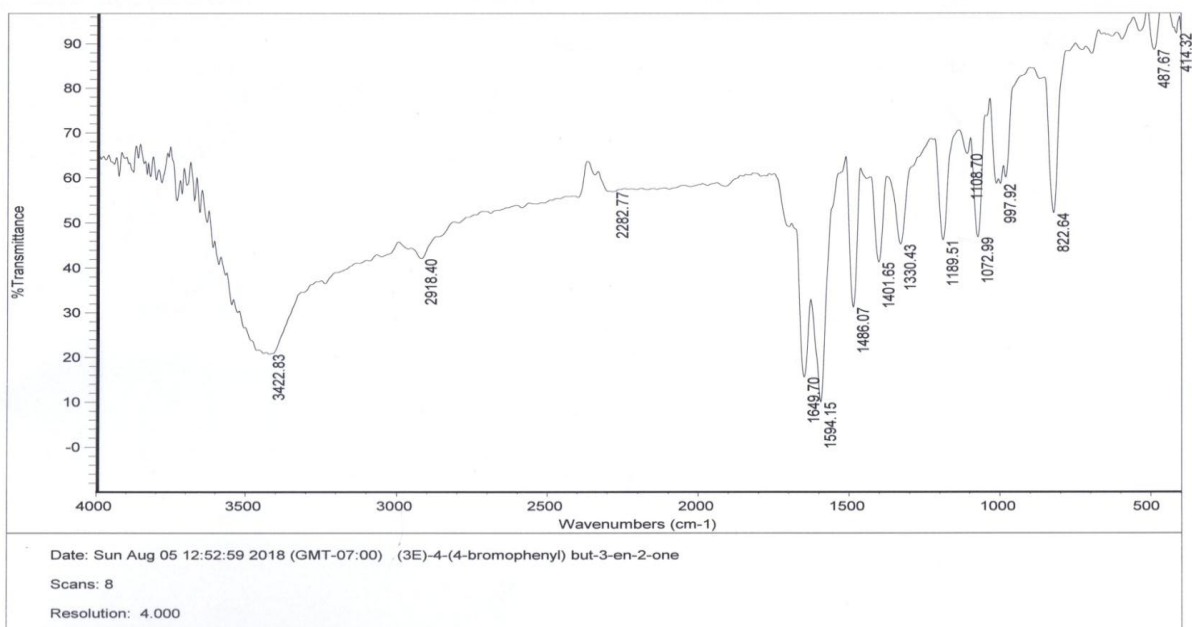


Figure (3.64) show the IR spectrum of compound VI



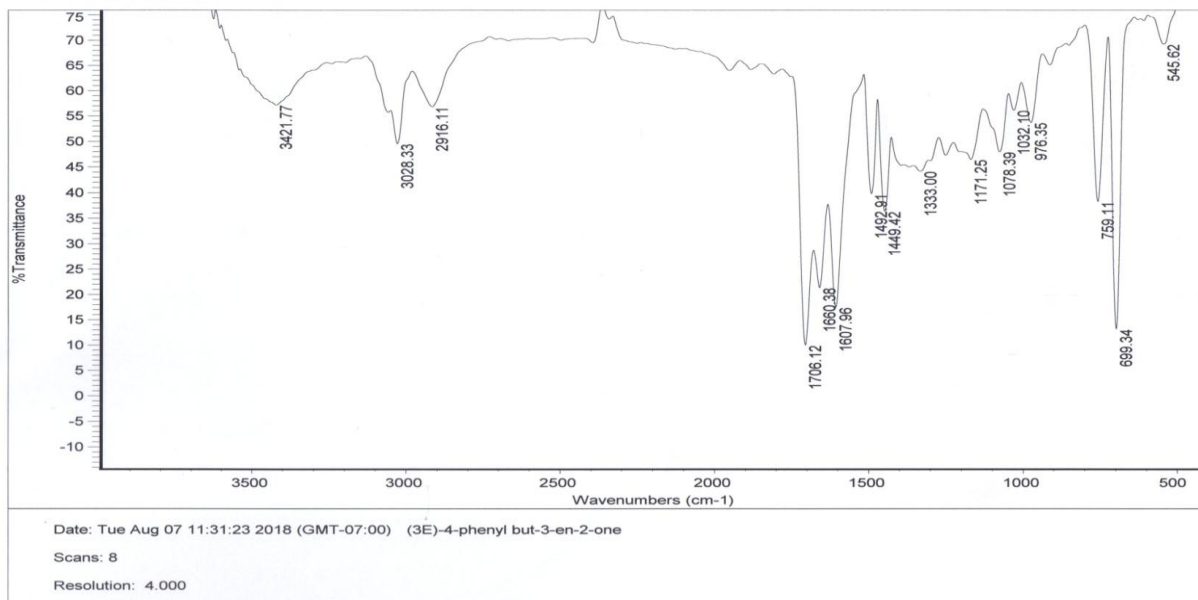


Figure (3.65) show the IR spectrum of compound VII

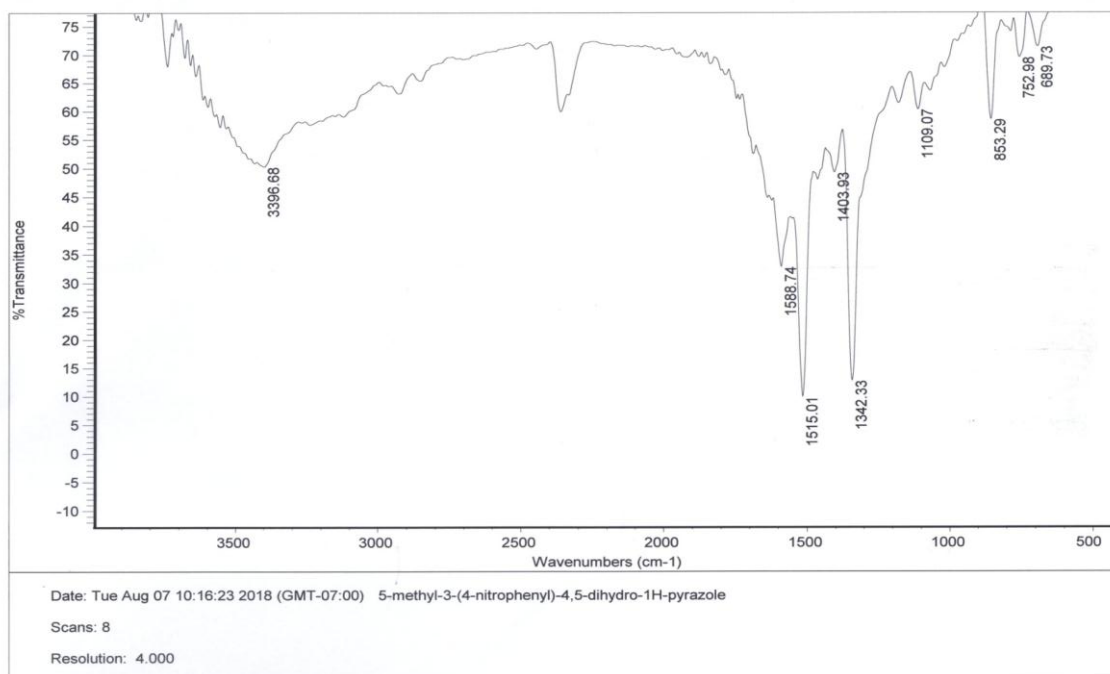


Figure (3.66) show the IR spectrum of compound VIII

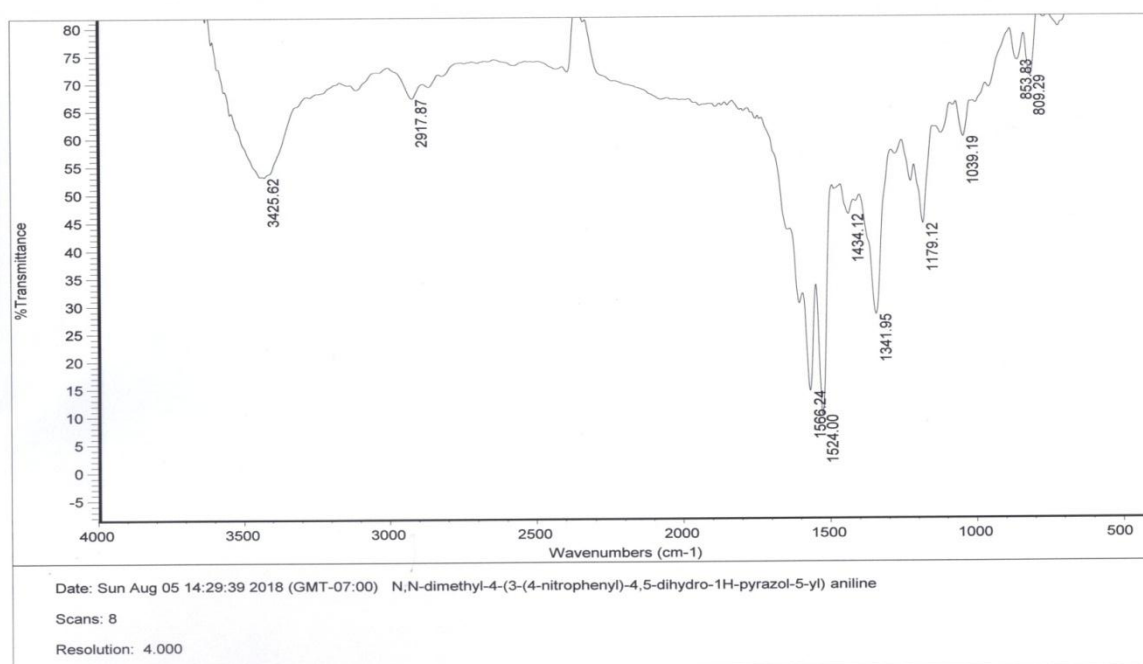


Figure (3.67) show the IR spectrum of compound IX

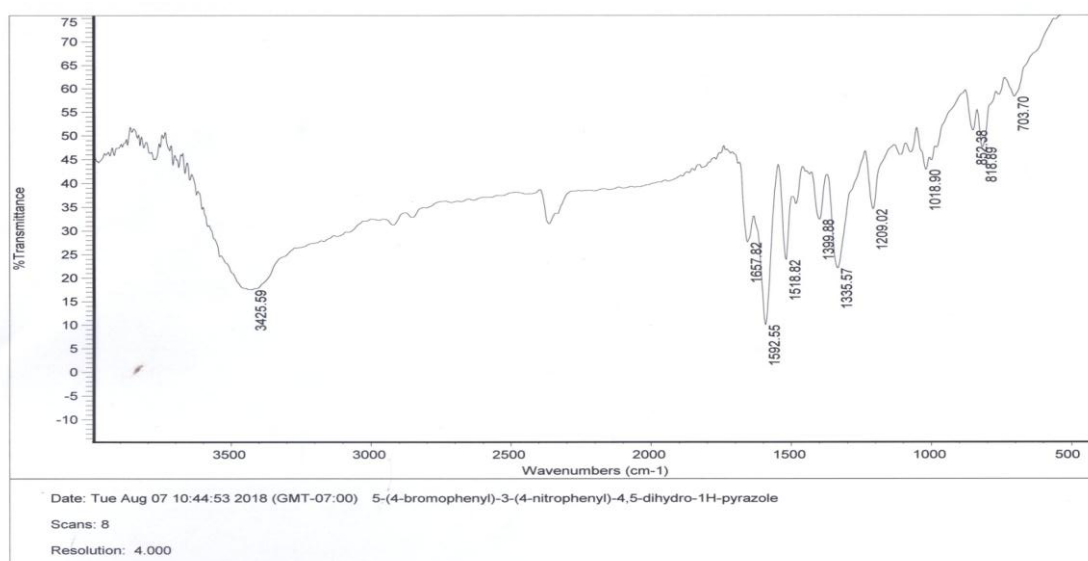


Figure (3.68) show the IR spectrum of compound X

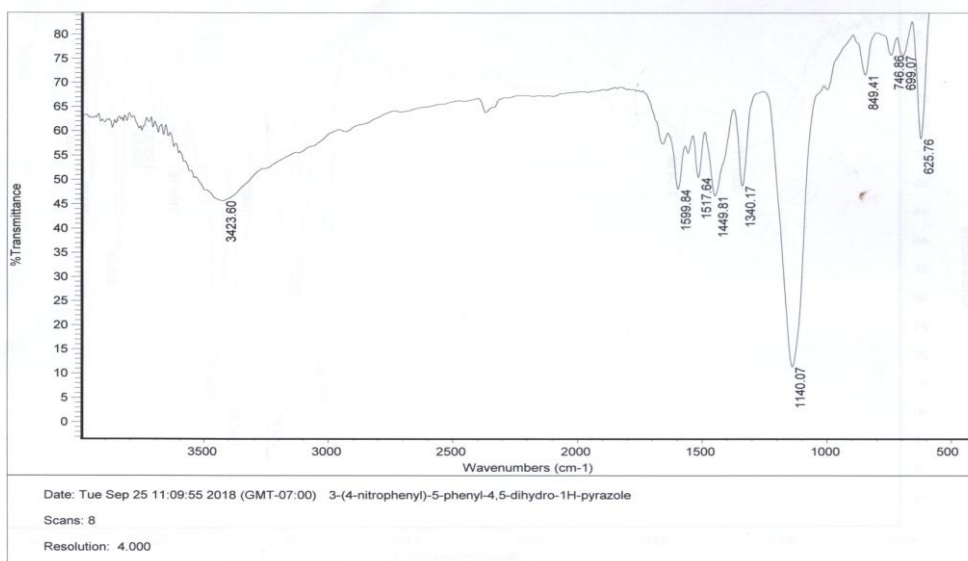


Figure (3.69) show the IR spectrum of compound XI

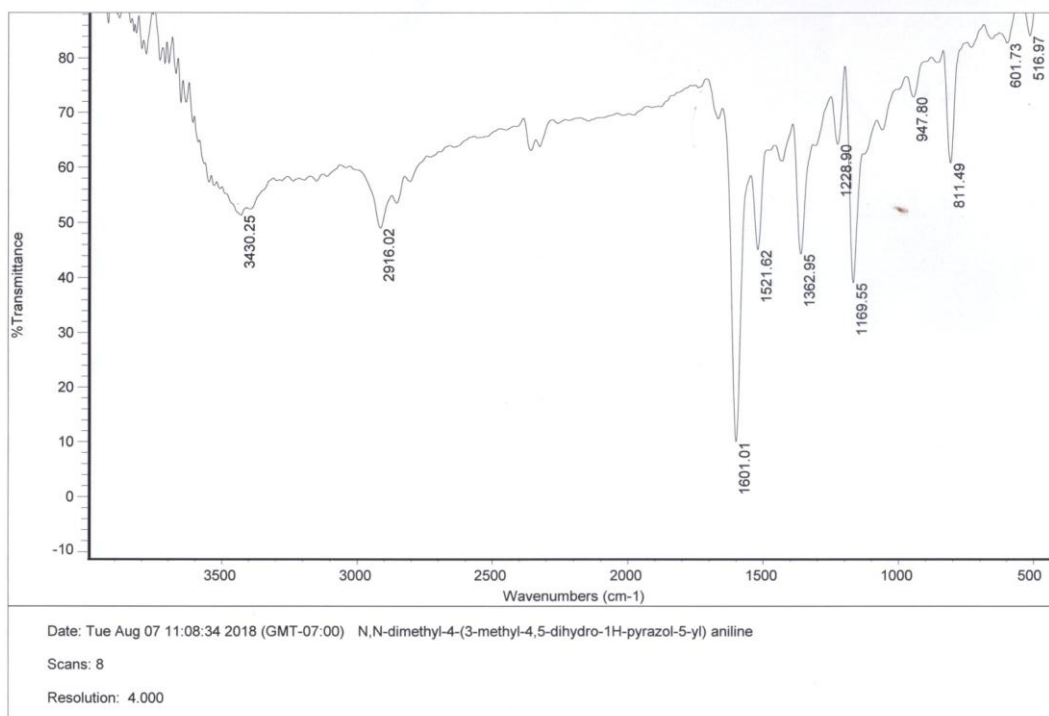
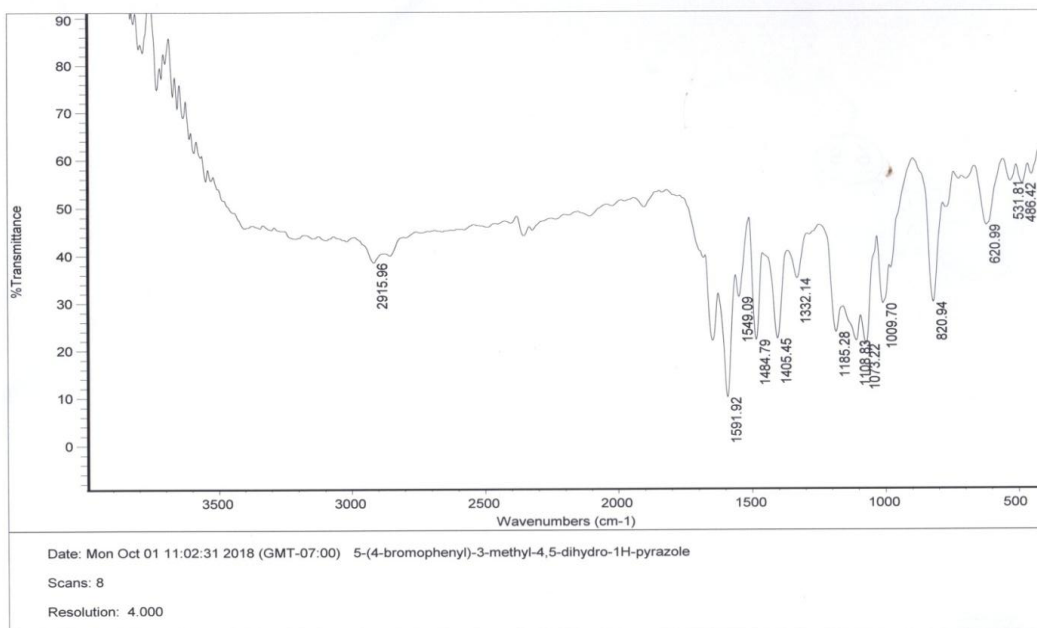
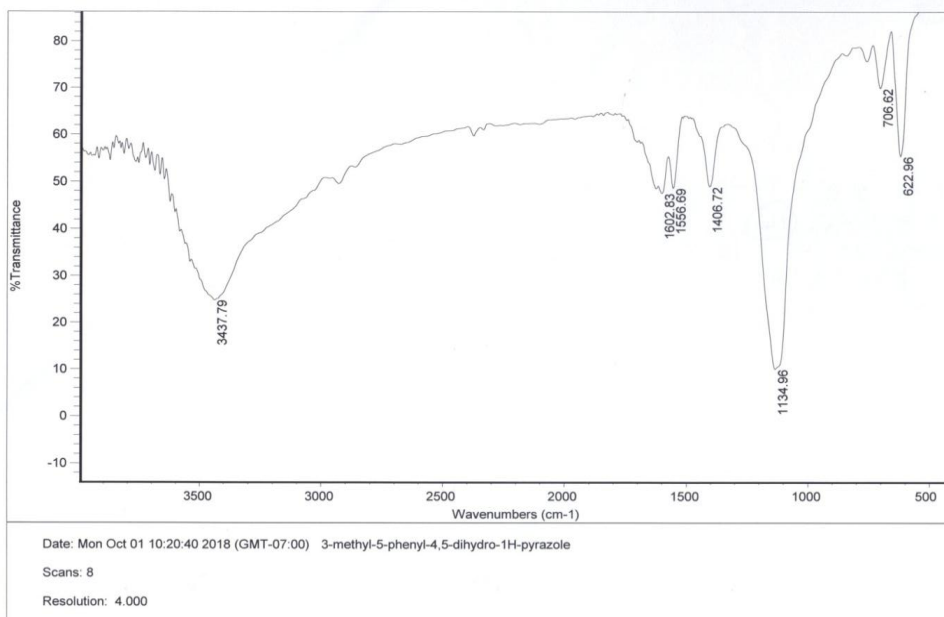


Figure (3.70) show the IR spectrum of compound XII



**Figure (3.71) show the IR spectrum of compound XIII**



**Figure (3.72) show the IR spectrum of compound XIV**